Preface

In these lecture notes, we will give a general introduction to the discontinuous Galerkin (DG) methods for solving time-dependent, convection-dominated partial differential equations (PDEs), including the hyperbolic conservation laws, convection-diffusion equations, and PDEs containing higher-order spatial derivatives such as the KdV equations and other nonlinear dispersive wave equations. We will discuss cell entropy inequalities, nonlinear stability, and error estimates. The important ingredient of the design of DG schemes, namely the adequate choice of numerical fluxes, will be explained in detail. Issues related to the implementation of the DG method will also be addressed.

Chapter 1

Introduction

Discontinuous Galerkin (DG) methods are a class of finite-element methods using completely discontinuous basis functions, which are usually chosen as piecewise polynomials. Since the basis functions can be completely discontinuous, these methods have the flexibility which is not shared by typical finite-element methods, such as the allowance of arbitrary triangulation with hanging nodes, complete freedom in changing the polynomial degrees in each element independent of that in the neighbors (p adaptivity), and extremely local data structure (elements only communicate with immediate neighbors regardless of the order of accuracy of the scheme) and the resulting embarrassingly high parallel efficiency (usually more than 99% for a fixed mesh, and more than 80% for a dynamic load balancing with adaptive meshes which change often during time evolution), see, e.g. [5]. A very good example to illustrate the capability of the discontinuous Galerkin method in h-p adaptivity, efficiency in parallel dynamic load balancing, and excellent resolution properties is the successful simulation of the Rayleigh-Taylor flow instabilities in [38].

The first discontinuous Galerkin method was introduced in 1973 by Reed and Hill [37], in the framework of neutron transport, i.e., a time-independent linear hyperbolic equation. A major development of the DG method is carried out by Cockburn et al. in a series of papers [14, 13, 12, 10, 15], in which they have established a framework to easily solve *nonlinear* time-dependent problems, such as the Euler equations of gas dynamics, using explicit, nonlinearly stable high-order Runge-Kutta time discretizations [44] and DG discretization in space with exact or approximate Riemann solvers as interface fluxes and total variation bounded (TVB) nonlinear limiters [41] to achieve non-oscillatory properties for strong shocks.

The DG method has found rapid applications in such diverse areas as aeroacoustics, electro-magnetism, gas dynamics, granular flows, magnetohydrodynamics, meteorology, modeling of shallow water, oceanography, oil recovery simulation, semiconductor device simulation, transport of contaminant in

porous media, turbomachinery, turbulent flows, viscoelastic flows and weather forecasting, among many others. For more details, we refer to the survey paper [11], and other papers in that Springer volume, which contains the conference proceedings of the First International Symposium on Discontinuous Galerkin Methods held at Newport, Rhode Island in 1999. The lecture notes [8] is a good reference for many details, as well as the extensive review paper [17]. More recently, there are two special issues devoted to the discontinuous Galerkin method [18, 19], which contain many interesting papers in the development of the method in all aspects including algorithm design, analysis, implementation and applications.

Chapter 2

Time Discretization

In these lecture notes, we will concentrate on the method of lines DG methods, that is, we do not discretize the time variable. Therefore, we will briefly discuss the issue of time discretization at the beginning.

For hyperbolic problems or convection-dominated problems such as Navier-Stokes equations with high Reynolds numbers, we often use a class of high-order nonlinearly stable Runge-Kutta time discretizations. A distinctive feature of this class of time discretizations is that they are convex combinations of first-order forward Euler steps, hence they maintain strong stability properties in any semi-norm (total variation semi-norm, maximum norm, entropy condition, etc.) of the forward Euler step. Thus one only needs to prove nonlinear stability for the first-order forward Euler step, which is relatively easy in many situations (e.g., TVD schemes, see for example Section 3.2.2 below), and one automatically obtains the same strong stability property for the higher-order time discretizations in this class. These methods were first developed in [44] and [42], and later generalized in [20] and [21]. The most popular scheme in this class is the following third-order Runge-Kutta method for solving

$$u_t = L(u,t)$$

where $L(u,t)$ is a spatial discretization operator (it does not need to be, and often is not, linear!):

$$\begin{aligned} u^{(1)} &= u^n + \Delta t L(u^n, t^n), \\ u^{(2)} &= \frac{3}{4}u^n + \frac{1}{4}u^{(1)} + \frac{1}{4}\Delta t L(u^{(1)}, t^n + \Delta t), \\ u^{n+1} &= \frac{1}{3}u^n + \frac{2}{3}u^{(2)} + \frac{2}{3}\Delta t L(u^{(2)}, t^n + \frac{1}{2}\Delta t). \end{aligned} \tag{2.1}$$

Schemes in this class which are higher order or are of low storage also exist. For details, see the survey paper [43] and the review paper [21].

If the PDEs contain high-order spatial derivatives with coefficients not very small, then explicit time marching methods such as the Runge-Kutta methods described above suffer from severe time-step restrictions. It is an important and active research subject to study efficient time discretization for such situations, while still maintaining the advantages of the DG methods, such as their local nature and parallel efficiency. See, e.g. [46] for a study of several time discretization techniques for such situations. We will not further discuss this important issue though in these lectures.

Chapter 3

Discontinuous Galerkin Method for Conservation Laws

The discontinuous Galerkin method was first designed as an effective numerical method for solving hyperbolic conservation laws, which may have discontinuous solutions. In this section we will discuss the algorithm formulation, stability analysis, and error estimates for the discontinuous Galerkin method solving hyperbolic conservation laws.

3.1 Two-dimensional Steady-State Linear Equations

We now present the details of the original DG method in [37] for the two-dimensional steady-state linear convection equation

$$au_x + bu_y = f(x, y), \qquad 0 \le x,\, y \le 1, \tag{3.1}$$

where a and b are constants. Without loss of generality we assume $a > 0$, $b > 0$. The equation (3.1) is well posed when equipped with the inflow boundary condition

$$u(x, 0) = g_1(x),\ \ 0 \le x \le 1 \qquad \text{and} \qquad u(0, y) = g_2(y),\ \ 0 \le y \le 1. \tag{3.2}$$

For simplicity, we assume a rectangular mesh to cover the computational domain $[0, 1]^2$, consisting of cells

$$I_{i,j} = \left\{(x, y) :\, x_{i-\frac{1}{2}} \le x \le x_{i+\frac{1}{2}},\ y_{j-\frac{1}{2}} \le y \le y_{j+\frac{1}{2}}\right\}$$

for $1 \le i \le N_x$ and $1 \le j \le N_y$, where

$$0 = x_{\frac{1}{2}} < x_{\frac{3}{2}} < \cdots < x_{N_x+\frac{1}{2}} = 1$$

and

$$0 = y_{\frac{1}{2}} < y_{\frac{3}{2}} < \cdots < y_{N_y+\frac{1}{2}} = 1$$

are discretizations in x and y over $[0,1]$. We also denote

$$\Delta x_i = x_{i+\frac{1}{2}} - x_{i-\frac{1}{2}},\ \ 1 \le i \le N_x; \qquad \Delta y_j = y_{j+\frac{1}{2}} - y_{j-\frac{1}{2}},\ \ 1 \le j \le N_y;$$

and

$$h = \max\left(\max_{1\le i\le N_x} \Delta x_i,\ \max_{1\le j\le N_y} \Delta y_j\right).$$

We assume the mesh is regular, namely there is a constant $c > 0$ independent of h such that

$$\Delta x_i \ge ch,\ \ 1 \le i \le N_x; \qquad \Delta y_j \ge ch,\ \ 1 \le j \le N_y.$$

We define a finite-element space consisting of piecewise polynomials

$$V_h^k = \left\{v : v|_{I_{i,j}} \in P^k(I_{i,j});\ 1 \le i \le N_x,\ 1 \le j \le N_y\right\}, \tag{3.3}$$

where $P^k(I_{i,j})$ denotes the set of polynomials of degree up to k defined on the cell $I_{i,j}$. Notice that functions in V_h^k may be discontinuous across cell interfaces.

The discontinuous Galerkin (DG) method for solving (3.1) is defined as follows: find the unique function $u_h \in V_h^k$ such that, for all test functions $v_h \in V_h^k$ and all $1 \le i \le N_x$ and $1 \le j \le N_y$, we have

$$\begin{aligned}
&-\int\int_{I_{i,j}} (au_h(v_h)_x + bu_h(v_h)_y)\,dxdy + a\int_{y_{j-\frac{1}{2}}}^{y_{j+\frac{1}{2}}} \widehat{u}_h(x_{i+\frac{1}{2}}, y)v_h(x^-_{i+\frac{1}{2}}, y)dy \\
&- a\int_{y_{j-\frac{1}{2}}}^{y_{j+\frac{1}{2}}} \widehat{u}_h(x_{i-\frac{1}{2}}, y)v_h(x^+_{i-\frac{1}{2}}, y)dy + b\int_{x_{i-\frac{1}{2}}}^{x_{i+\frac{1}{2}}} \widehat{u}_h(x, y_{j+\frac{1}{2}})v_h(x, y^-_{j+\frac{1}{2}})dx \\
&- b\int_{x_{i-\frac{1}{2}}}^{x_{i+\frac{1}{2}}} \widehat{u}_h(x, y_{j-\frac{1}{2}})v_h(x, y^+_{j-\frac{1}{2}})dx = \int\int_{I_{i,j}} f\,v_h\,dxdy.
\end{aligned} \tag{3.4}$$

Here, $\widehat{u}_h$ is the so-called "numerical flux", which is a single-valued function defined at the cell interfaces and in general depending on the values of the numerical solution u_h from both sides of the interface, since u_h is discontinuous there. For the simple linear convection PDE (3.1), the numerical flux can be chosen according to the upwind principle, namely

$$\widehat{u}_h(x_{i+\frac{1}{2}}, y) = u_h(x^-_{i+\frac{1}{2}}, y), \qquad \widehat{u}_h(x, y_{j+\frac{1}{2}}) = u_h(x, y^-_{j+\frac{1}{2}}).$$

Notice that, for the boundary cell $i = 1$, the numerical flux for the left edge is defined using the given boundary condition

$$\widehat{u}_h(x_{\frac{1}{2}}, y) = g_2(y).$$

Likewise, for the boundary cell $j = 1$, the numerical flux for the bottom edge is defined by

$$\widehat{u}_h(x, y_{\frac{1}{2}}) = g_1(x).$$

We now look at the implementation of the scheme (3.4). If a local basis of $P^k(I_{i,j})$ is chosen and denoted as $\varphi^\ell_{i,j}(x, y)$ for $\ell = 1, 2, \ldots, K = (k + 1)(k + 2)/2$, we can express the numerical solution as

$$u_h(x, y) = \sum_{\ell=1}^{K} u^\ell_{i,j} \varphi^\ell_{i,j}(x, y), \qquad (x, y) \in I_{i,j},$$

and we should solve for the coefficients

$$u_{i,j} = \begin{pmatrix} u^1_{i,j} \\ \vdots \\ u^K_{i,j} \end{pmatrix},$$

which, according to the scheme (3.4), satisfies the linear equation

$$A_{i,j} u_{i,j} = rhs \tag{3.5}$$

where $A_{i,j}$ is a $K \times K$ matrix whose (ℓ, m)-th entry is given by

$$\begin{aligned} a^{\ell,m}_{i,j} = &- \int\int_{I_{i,j}} \left(a\varphi^m_{i,j}(x, y)(\varphi^\ell_{i,j}(x, y))_x + b\varphi^m_{i,j}(x, y)(\varphi^\ell_{i,j}(x, y))_y \right) dxdy \\ &+ a \int_{y_{j-\frac{1}{2}}}^{y_{j+\frac{1}{2}}} \varphi^m_{i,j}(x_{i+\frac{1}{2}}, y)\varphi^\ell_{i,j}(x_{i+\frac{1}{2}}, y)dy \\ &+ b \int_{x_{i-\frac{1}{2}}}^{x_{i+\frac{1}{2}}} \varphi^m_{i,j}(x, y_{j+\frac{1}{2}})\varphi^\ell_{i,j}(x, y_{j+\frac{1}{2}})dx, \end{aligned} \tag{3.6}$$

and the ℓ-th entry of the right-hand side vector is given by

$$\begin{aligned} rhs^\ell = &\, a \int_{y_{j-\frac{1}{2}}}^{y_{j+\frac{1}{2}}} u_h(x^-_{i-\frac{1}{2}}, y)\varphi^\ell_{i,j}(x_{i-\frac{1}{2}}, y)dy + b \int_{x_{i-\frac{1}{2}}}^{x_{i+\frac{1}{2}}} u_h(x, y^-_{j-\frac{1}{2}})\varphi^\ell_{i,j}(x, y_{j-\frac{1}{2}})dx \\ &+ \int_{I_{i,j}} f\, \varphi^\ell_{i,j}\, dxdy, \end{aligned}$$

which depends on the information of u_h in the left cell $I_{i-1,j}$ and the bottom cell $I_{i,j-1}$, if they are in the computational domain, or on the boundary condition, if one or both of these cells are outside the computational domain. It is easy to verify that the matrix $A_{i,j}$ in (3.5) with entries given by (3.6) is invertible, hence the numerical solution u_h in the cell $I_{i,j}$ can be easily obtained by solving the small linear system (3.5), once the solution at the left and bottom cells $I_{i-1,j}$

and $I_{i,j-1}$ are already known, or if one or both of these cells are outside the computational domain. Therefore, we can obtain the numerical solution u_h in the following ordering: first we obtain it in the cell $I_{1,1}$, since both its left and bottom boundaries are equipped with the prescribed boundary conditions (3.2). We then obtain the solution in the cells $I_{2,1}$ and $I_{1,2}$. For $I_{2,1}$, the numerical solution u_h in its left cell $I_{1,1}$ is already available, and its bottom boundary is equipped with the prescribed boundary condition (3.2). Similar argument goes for the cell $I_{1,2}$. The next group of cells to be solved are $I_{3,1}$, $I_{2,2}$, $I_{1,3}$. It is clear that we can obtain the solution u_h sequentially in this way for all cells in the computational domain.

Clearly, this method does not involve any large system solvers and is very easy to implement. In [25], Lesaint and Raviart proved that this method is convergent with the optimal order of accuracy, namely $O(h^{k+1})$, in L^2-norm, when piecewise tensor product polynomials of degree k are used as basis functions. Numerical experiments indicate that the convergence rate is also optimal when the usual piecewise polynomials of degree k given by (3.3) are used instead.

Notice that, even though the method (3.4) is designed for the steady-state problem (3.1), it can be easily used on initial-boundary value problems of linear time-dependent hyperbolic equations: we just need to identify the time variable t as one of the spatial variables. It is also easily generalizable to higher dimensions.

The method described above can be easily designed and efficiently implemented on arbitrary triangulations. L^2-error estimates of $O(h^{k+1/2})$ where k is again the polynomial degree and h is the mesh size can be obtained when the solution is sufficiently smooth, for arbitrary meshes, see, e.g., [24]. This estimate is actually sharp for the most general situation [33], however in many cases the optimal $O(h^{k+1})$ error bound can be proved [39, 9]. In actual numerical computations, one almost always observes the optimal $O(h^{k+1})$ accuracy.

Unfortunately, even though the method (3.4) is easy to implement, accurate, and efficient, it cannot be easily generalized to linear systems, where the characteristic information comes from different directions, or to nonlinear problems, where the characteristic wind direction depends on the solution itself.

3.2 One-dimensional Time-dependent Conservation Laws

The difficulties mentioned at the end of the last subsection can be by-passed when the DG discretization is only used for the spatial variables, and the time discretization is achieved by explicit Runge-Kutta methods such as (2.1). This is the approach of the so-called Runge-Kutta discontinuous Galerkin (RKDG) method [14, 13, 12, 10, 15].

We start our discussion with the one-dimensional conservation law

$$u_t + f(u)_x = 0. \tag{3.7}$$

As before, we assume the following mesh to cover the computational domain $[0,1]$, consisting of cells $I_i = [x_{i-\frac{1}{2}}, x_{i+\frac{1}{2}}]$, for $1 \le i \le N$, where

$$0 = x_{\frac{1}{2}} < x_{\frac{3}{2}} < \cdots < x_{N+\frac{1}{2}} = 1.$$

We again denote

$$\Delta x_i = x_{i+\frac{1}{2}} - x_{i-\frac{1}{2}}, \ \ 1 \le i \le N; \qquad h = \max_{1\le i\le N} \Delta x_i.$$

We assume the mesh is regular, namely there is a constant $c > 0$ independent of h such that

$$\Delta x_i \ge ch, \qquad 1 \le i \le N.$$

We define a finite-element space consisting of piecewise polynomials

$$V_h^k = \left\{ v : v|_{I_i} \in P^k(I_i); \ 1 \le i \le N \right\}, \tag{3.8}$$

where $P^k(I_i)$ denotes the set of polynomials of degree up to k defined on the cell I_i. The semi-discrete DG method for solving (3.7) is defined as follows: find the unique function $u_h = u_h(t) \in V_h^k$ such that, for all test functions $v_h \in V_h^k$ and all $1 \le i \le N$, we have

$$\int_{I_i} (u_h)_t (v_h) dx - \int_{I_i} f(u_h)(v_h)_x dx + \widehat{f}_{i+\frac{1}{2}} v_h(x^-_{i+\frac{1}{2}}) - \widehat{f}_{i-\frac{1}{2}} v_h(x^+_{i-\frac{1}{2}}) = 0. \tag{3.9}$$

Here, $\widehat{f}_{i+\frac{1}{2}}$ is again the numerical flux, which is a single-valued function defined at the cell interfaces and in general depends on the values of the numerical solution u_h from both sides of the interface

$$\widehat{f}_{i+\frac{1}{2}} = \widehat{f}(u_h(x^-_{i+\frac{1}{2}}, t), u_h(x^+_{i+\frac{1}{2}}, t)).$$

We use the so-called monotone fluxes from finite-difference and finite-volume schemes for solving conservation laws, which satisfy the following conditions:

- Consistency: $\widehat{f}(u,u) = f(u)$.
- Continuity: $\widehat{f}(u^-, u^+)$ is at least Lipschitz continuous with respect to both arguments u^- and u^+.
- Monotonicity: $\widehat{f}(u^-, u^+)$ is a non-decreasing function of its first argument u^- and a non-increasing function of its second argument u^+. Symbolically $\widehat{f}(\uparrow, \downarrow)$.

Well-known monotone fluxes include the Lax-Friedrichs flux

$$\widehat{f}^{LF}(u^-, u^+) = \frac{1}{2}\left(f(u^-) + f(u^+) - \alpha(u^+ - u^-) \right), \qquad \alpha = \max_u |f'(u)|;$$

the Godunov flux

$$\widehat{f}^{God}(u^-,u^+)=\begin{cases}\min_{u^-\le u\le u^+} f(u), & \text{if } u^-<u^+,\\ \max_{u^+\le u\le u^-} f(u), & \text{if } u^-\ge u^+;\end{cases}$$

and the Engquist-Osher flux

$$\widehat{f}^{EO}=\int_0^{u^-}\max(f'(u),0)du+\int_0^{u^+}\min(f'(u),0)du+f(0).$$

We refer to, e.g., [26] for more details about monotone fluxes.

3.2.1 Cell Entropy Inequality and L^2-Stability

It is well known that weak solutions of (3.7) may not be unique and the unique, physically relevant weak solution (the so-called entropy solution) satisfies the following entropy inequality

$$U(u)_t+F(u)_x\le 0 \tag{3.10}$$

in distribution sense, for any convex entropy $U(u)$ satisfying $U''(u)\ge 0$ and the corresponding entropy flux $F(u)=\int^u U'(u)f'(u)du$. It will be nice if a numerical approximation to (3.7) also shares a similar entropy inequality as (3.10). It is usually quite difficult to prove a discrete entropy inequality for finite-difference or finite-volume schemes, especially for high-order schemes and when the flux function $f(u)$ in (3.7) is not convex or concave, see, e.g., [28, 32]. However, it turns out that it is easy to prove that the DG scheme (3.9) satisfies a cell entropy inequality [23].

Proposition 3.1. *The solution u_h to the semi-discrete DG scheme* (3.9) *satisfies the following cell entropy inequality*

$$\frac{d}{dt}\int_{I_i}U(u_h)\,dx+\widehat{F}_{i+\frac12}-\widehat{F}_{i-\frac12}\le 0 \tag{3.11}$$

for the square entropy $U(u)=\frac{u^2}{2}$, for some consistent entropy flux

$$\widehat{F}_{i+\frac12}=\widehat{F}(u_h(x^-_{i+\frac12},t),u_h(x^+_{i+\frac12},t))$$

satisfying $\widehat{F}(u,u)=F(u)$.

Proof. We introduce a short-hand notation

$$B_i(u_h;v_h)=\int_{I_i}(u_h)_t(v_h)dx-\int_{I_i}f(u_h)(v_h)_x dx + \widehat{f}_{i+\frac12}v_h(x^-_{i+\frac12})-\widehat{f}_{i-\frac12}v_h(x^+_{i-\frac12}). \tag{3.12}$$

If we take $v_h = u_h$ in the scheme (3.9), we obtain

$$B_i(u_h;u_h)=\int_{I_i}(u_h)_t(u_h)dx-\int_{I_i}f(u_h)(u_h)_x dx + \widehat{f}_{i+\frac{1}{2}}u_h(x^-_{i+\frac{1}{2}})-\widehat{f}_{i-\frac{1}{2}}u_h(x^+_{i-\frac{1}{2}})=0. \quad (3.13)$$

If we denote $\widetilde{F}(u)=\int^u f(u)du$, then (3.13) becomes

$$B_i(u_h;u_h)=\int_{I_i}U(u_h)_t dx-\widetilde{F}(u_h(x^-_{i+\frac{1}{2}})) + \widetilde{F}(u_h(x^+_{i-\frac{1}{2}}))+\widehat{f}_{i+\frac{1}{2}}u_h(x^-_{i+\frac{1}{2}})-\widehat{f}_{i-\frac{1}{2}}u_h(x^+_{i-\frac{1}{2}})=0,$$

or

$$B_i(u_h;u_h)=\int_{I_i}U(u_h)_t dx+\widehat{F}_{i+\frac{1}{2}}-\widehat{F}_{i-\frac{1}{2}}+\Theta_{i-\frac{1}{2}}=0, \quad (3.14)$$

where

$$\widehat{F}_{i+\frac{1}{2}}=-\widetilde{F}(u_h(x^-_{i+\frac{1}{2}}))+\widehat{f}_{i+\frac{1}{2}}u_h(x^-_{i+\frac{1}{2}}), \quad (3.15)$$

and

$$\Theta_{i-\frac{1}{2}}=-\widetilde{F}(u_h(x^-_{i-\frac{1}{2}}))+\widehat{f}_{i-\frac{1}{2}}u_h(x^-_{i-\frac{1}{2}})+\widetilde{F}(u_h(x^+_{i-\frac{1}{2}}))-\widehat{f}_{i-\frac{1}{2}}u_h(x^+_{i-\frac{1}{2}}). \quad (3.16)$$

It is easy to verify that the numerical entropy flux $\widehat{F}$ defined by (3.15) is consistent with the entropy flux $F(u)=\int^u U'(u)f'(u)du$ for $U(u)=\frac{u^2}{2}$. It is also easy to verify

$$\Theta=-\widetilde{F}(u_h^-)+\widehat{f}u_h^-+\widetilde{F}(u_h^+)-\widehat{f}u_h^+=(u_h^+-u_h^-)(\widetilde{F}'(\xi)-\widehat{f})\geq 0,$$

where we have dropped the subscript $i-\frac{1}{2}$ since all quantities are evaluated there in $\Theta_{i-\frac{1}{2}}$. A mean value theorem is applied and ξ is a value between u^- and u^+, and we have used the fact $\widetilde{F}'(\xi)=f(\xi)$ and the monotonicity of the flux function $\widehat{f}$ to obtain the last inequality. This finishes the proof of the cell entropy inequality (3.11). □

We note that the proof does not depend on the accuracy of the scheme, namely it holds for the piecewise polynomial space (3.8) with any degree k. Also, the same proof can be given for the multi-dimensional DG scheme on any triangulation.

The cell entropy inequality trivially implies an L^2-stability of the numerical solution.

Proposition 3.2. *For periodic or compactly supported boundary conditions, the solution u_h to the semi-discrete* DG *scheme* (3.9) *satisfies the following L^2-stability*

$$\frac{d}{dt}\int_0^1(u_h)^2dx\leq 0, \quad (3.17)$$

or

$$\|u_h(\cdot,t)\| \le \|u_h(\cdot,0)\|. \tag{3.18}$$

Here and below, an unmarked norm is the usual L^2-norm.

Proof. We simply sum up the cell entropy inequality (3.11) over i. The flux terms telescope and there is no boundary term left because of the periodic or compact supported boundary condition. (3.17), and hence (3.18), are now immediate. □

Notice that both the cell entropy inequality (3.11) and the L^2-stability (3.17) are valid even when the exact solution of the conservation law (3.7) is discontinuous.

3.2.2 Limiters and Total Variation Stability

For discontinuous solutions, the cell entropy inequality (3.11) and the L^2-stability (3.17), although helpful, are not enough to control spurious numerical oscillations near discontinuities. In practice, especially for problems containing strong discontinuities, we often need to apply nonlinear limiters to control these oscillations and to obtain provable total variation stability.

For simplicity, we first consider the forward Euler time discretization of the semi-discrete DG scheme (3.9). Starting from a preliminary solution $u_h^{n,\mathrm{pre}} \in V_h^k$ at time level n (for the initial condition, $u_h^{0,\mathrm{pre}}$ is taken to be the L^2-projection of the analytical initial condition $u(\cdot,0)$ into V_h^k), we would like to "limit" or "preprocess" it to obtain a new function $u_h^n \in V_h^k$ before advancing it to the next time level: find $u_h^{n+1,\mathrm{pre}} \in V_h^k$ such that, for all test functions $v_h \in V_h^k$ and all $1 \le i \le N$, we have

$$\int_{I_i} \frac{u_h^{n+1,\mathrm{pre}} - u_h^n}{\Delta t} v_h dx - \int_{I_i} f(u_h^n)(v_h)_x dx + \widehat{f}^n_{i+\frac{1}{2}} v_h(x^-_{i+\frac{1}{2}}) - \widehat{f}^n_{i-\frac{1}{2}} v_h(x^+_{i-\frac{1}{2}}) = 0, \tag{3.19}$$

where $\Delta t = t^{n+1} - t^n$ is the time step. This limiting procedure to go from $u_h^{n,\mathrm{pre}}$ to u_h^n should satisfy the following two conditions:

- It should not change the cell averages of $u_h^{n,\mathrm{pre}}$. That is, the cell averages of u_h^n and $u_h^{n,\mathrm{pre}}$ are the same. This is for the conservation property of the DG method.
- It should not affect the accuracy of the scheme in smooth regions. That is, in the smooth regions this limiter does not change the solution, $u_h^n(x) = u_h^{n,\mathrm{pre}}(x)$.

There are many limiters discussed in the literature, and this is still an active research area, especially for multi-dimensional systems, see, e.g., [60]. We will only present an example [13] here.

We denote the cell average of the solution u_h as

$$\bar{u}_i = \frac{1}{\Delta x_i} \int_{I_i} u_h dx, \tag{3.20}$$

and we further denote

$$\widetilde{u}_i = u_h(x^-_{i+\frac{1}{2}}) - \bar{u}_i, \qquad \widetilde{\widetilde{u}}_i = \bar{u}_i - u_h(x^+_{i-\frac{1}{2}}). \tag{3.21}$$

The limiter should not change $\bar{u}_i$ but it may change $\widetilde{u}_i$ and/or $\widetilde{\widetilde{u}}_i$. In particular, the minmod limiter [13] changes $\widetilde{u}_i$ and $\widetilde{\widetilde{u}}_i$ into

$$\widetilde{u}_i^{(\mathrm{mod})} = m(\widetilde{u}_i, \Delta_+\bar{u}_i, \Delta_-\bar{u}_i), \qquad \widetilde{\widetilde{u}}_i^{(\mathrm{mod})} = m(\widetilde{\widetilde{u}}_i, \Delta_+\bar{u}_i, \Delta_-\bar{u}_i), \tag{3.22}$$

where

$$\Delta_+\bar{u}_i = \bar{u}_{i+1} - \bar{u}_i, \qquad \Delta_-\bar{u}_i = \bar{u}_i - \bar{u}_{i-1},$$

and the minmod function m is defined by

$$m(a_1, \cdots, a_\ell) = \begin{cases} s \, \min(|a_1|, \cdots, |a_\ell|), & \text{if } s = \mathrm{sign}(a_1) = \cdots \mathrm{sign}(a_\ell), \\ 0, & \text{otherwise.} \end{cases} \tag{3.23}$$

The limited function $u_h^{(\mathrm{mod})}$ is then recovered to maintain the old cell average (3.20) and the new point values given by (3.22), that is

$$u_h^{(\mathrm{mod})}(x^-_{i+\frac{1}{2}}) = \bar{u}_i + \widetilde{u}_i^{(\mathrm{mod})}, \qquad u_h^{(\mathrm{mod})}(x^+_{i-\frac{1}{2}}) = \bar{u}_i - \widetilde{\widetilde{u}}_i^{(\mathrm{mod})}, \tag{3.24}$$

by the definition (3.21). This recovery is unique for P^k polynomials with $k \le 2$. For $k > 2$, we have extra freedom in obtaining $u_h^{(\mathrm{mod})}$. We could for example choose $u_h^{(\mathrm{mod})}$ to be the unique P^2 polynomial satisfying (3.20) and (3.24).

Before discussing the total variation stability of the DG scheme (3.19) with the pre-processing, we first present a simple lemma due to Harten [22].

Lemma 3.1 (Harten). *If a scheme can be written in the form*

$$u_i^{n+1} = u_i^n + C_{i+\frac{1}{2}}\Delta_+ u_i^n - D_{i-\frac{1}{2}}\Delta_- u_i^n \tag{3.25}$$

with periodic or compactly supported boundary conditions, where $C_{i+\frac{1}{2}}$ and $D_{i-\frac{1}{2}}$ may be nonlinear functions of the grid values u_j^n for $j = i-p, \ldots, i+q$ with some $p, q \ge 0$, satisfying

$$C_{i+\frac{1}{2}} \ge 0, \qquad D_{i+\frac{1}{2}} \ge 0, \qquad C_{i+\frac{1}{2}} + D_{i+\frac{1}{2}} \le 1, \qquad \forall i, \tag{3.26}$$

then the scheme is TVD

$$TV(u^{n+1}) \le TV(u^n),$$

where the total variation seminorm is defined by

$$TV(u) = \sum_i |\Delta_+ u_i|.$$

Proof. Taking the forward difference operation on (3.25) yields

$$\begin{aligned}\Delta_+ u_i^{n+1} &= \Delta_+ u_i^n + C_{i+\frac{3}{2}}\Delta_+ u_{i+1}^n - C_{i+\frac{1}{2}}\Delta_+ u_i^n - D_{i+\frac{1}{2}}\Delta_+ u_i^n + D_{i-\frac{1}{2}}\Delta_- u_i^n \\ &= (1 - C_{i+\frac{1}{2}} - D_{i+\frac{1}{2}})\Delta_+ u_i^n + C_{i+\frac{3}{2}}\Delta_+ u_{i+1}^n + D_{i-\frac{1}{2}}\Delta_- u_i^n.\end{aligned}$$

Thanks to (3.26) and using the periodic or compactly supported boundary condition, we can take the absolute value on both sides of the above equality and sum up over i to obtain

$$\begin{aligned}\sum_i |\Delta_+ u_i^{n+1}| \le \sum_i (1 - C_{i+\frac{1}{2}} - D_{i+\frac{1}{2}})|\Delta_+ u_i^n| \\ + \sum_i C_{i+\frac{1}{2}}|\Delta_+ u_i^n| + \sum_i D_{i+\frac{1}{2}}|\Delta_+ u_i^n| = \sum_i |\Delta_+ u_i^n|.\end{aligned}$$

This finishes the proof. □

We define the "total variation in the means" semi-norm, or TVM, as

$$\mathrm{TVM}(u_h) = \sum_i |\Delta_+ \bar{u}_i|.$$

We then have the following stability result.

Proposition 3.3. *For periodic or compactly supported boundary conditions, the solution u_h^n of the DG scheme* (3.19)*, with the "pre-processing" by the limiter, is total variation diminishing in the means* (TVDM)*, that is*

$$\mathrm{TVM}(u_h^{n+1}) \le \mathrm{TVM}(u_h^n). \tag{3.27}$$

Proof. Taking $v_h = 1$ for $x \in I_i$ in (3.19) and dividing both sides by Δx_i, we obtain, by noticing (3.24),

$$\bar{u}_i^{n+1,\mathrm{pre}} = \bar{u}_i - \lambda_i \left(\widehat{f}(\bar{u}_i + \widetilde{u}_i, \bar{u}_{i+1} - \widetilde{\bar{u}}_{i+1}) - \widehat{f}(\bar{u}_{i-1} + \widetilde{u}_{i-1}, \bar{u}_i - \widetilde{\bar{u}}_i) \right),$$

where $\lambda_i = \frac{\Delta t}{\Delta x_i}$, and all quantities on the right-hand side are at the time level n. We can write the right hand side of the above equality in the Harten form (3.25) if we define $C_{i+\frac{1}{2}}$ and $D_{i-\frac{1}{2}}$ as follows

$$\begin{aligned}C_{i+\frac{1}{2}} &= -\lambda_i \frac{\widehat{f}(\bar{u}_i + \widetilde{u}_i, \bar{u}_{i+1} - \widetilde{\bar{u}}_{i+1}) - \widehat{f}(\bar{u}_i + \widetilde{u}_i, \bar{u}_i - \widetilde{\bar{u}}_i)}{\Delta_+ \bar{u}_i}, \\ D_{i-\frac{1}{2}} &= \lambda_i \frac{\widehat{f}(\bar{u}_i + \widetilde{u}_i, \bar{u}_i - \widetilde{\bar{u}}_i) - \widehat{f}(\bar{u}_{i-1} + \widetilde{u}_{i-1}, \bar{u}_i - \widetilde{\bar{u}}_i)}{\Delta_- \bar{u}_i}.\end{aligned} \tag{3.28}$$

We now need to verify that $C_{i+\frac{1}{2}}$ and $D_{i-\frac{1}{2}}$ defined in (3.28) satisfy (3.26). Indeed, we can write $C_{i+\frac{1}{2}}$ as

$$C_{i+\frac{1}{2}} = -\lambda_i \widehat{f}_2 \left[1 - \frac{\widetilde{\bar{u}}_{i+1}}{\Delta_+ \bar{u}_i} + \frac{\widetilde{\bar{u}}_i}{\Delta_+ \bar{u}_i} \right], \tag{3.29}$$

in which $\widehat{f}_2$ is defined as

$$\widehat{f}_2 = \frac{\widehat{f}(\bar{u}_i + \widetilde{u}_i, \bar{u}_{i+1} - \widetilde{\widetilde{u}}_{i+1}) - \widehat{f}(\bar{u}_i + \widetilde{u}_i, \bar{u}_i - \widetilde{\widetilde{u}}_i)}{(\bar{u}_{i+1} - \widetilde{\widetilde{u}}_{i+1}) - (\bar{u}_i - \widetilde{\widetilde{u}}_i)},$$

and hence

$$0 \le -\lambda_i \widehat{f}_2 = -\lambda_i \frac{\widehat{f}(\bar{u}_i + \widetilde{u}_i, \bar{u}_{i+1} - \widetilde{\widetilde{u}}_{i+1}) - \widehat{f}(\bar{u}_i + \widetilde{u}_i, \bar{u}_i - \widetilde{\widetilde{u}}_i)}{(\bar{u}_{i+1} - \widetilde{\widetilde{u}}_{i+1}) - (\bar{u}_i - \widetilde{\widetilde{u}}_i)} \le \lambda_i L_2, \quad (3.30)$$

where we have used the monotonicity and Lipschitz continuity of $\widehat{f}$, and L_2 is the Lipschitz constant of $\widehat{f}$ with respect to its second argument. Also, since u_h^n is the pre-processed solution by the minmod limiter, $\widetilde{\widetilde{u}}_{i+1}$ and $\widetilde{\widetilde{u}}_i$ are the modified values defined by (3.22), hence

$$0 \le \frac{\widetilde{\widetilde{u}}_{i+1}}{\Delta_+ \bar{u}_i} \le 1, \qquad 0 \le \frac{\widetilde{\widetilde{u}}_i}{\Delta_+ \bar{u}_i} \le 1. \quad (3.31)$$

Therefore, we have, by (3.29), (3.30) and (3.31),

$$0 \le C_{i+\frac{1}{2}} \le 2\lambda_i L_2.$$

Similarly, we can show that

$$0 \le D_{i+\frac{1}{2}} \le 2\lambda_{i+1} L_1$$

where L_1 is the Lipschitz constant of $\widehat{f}$ with respect to its first argument. This proves (3.26) if we take the time step so that

$$\lambda \le \frac{1}{2(L_1 + L_2)}$$

where $\lambda = \max_i \lambda_i$. The TVDM property (3.27) then follows from the Harten Lemma and the fact that the limiter does not change cell averages, hence $\mathrm{TVM}(u_h^{n+1}) = \mathrm{TVM}(u_h^{n+1,pre})$. □

Even though the previous proposition is proved only for the first-order Euler forward time discretization, the special TVD (or strong stability preserving, SSP) Runge-Kutta time discretizations [44, 21] allow us to obtain the same stability result for the fully discretized RKDG schemes.

Proposition 3.4. *Under the same conditions as those in Proposition* 3.3*, the solution* u_h^n *of the* DG *scheme* (3.19)*, with the Euler forward time discretization replaced by any* SSP *Runge-Kutta time discretization* [21] *such as* (2.1)*, is* TVDM. □

We still need to verify that the limiter (3.22) does not affect accuracy in smooth regions. If u_h is an approximation to a (locally) smooth function u, then a simple Taylor expansion gives

$$\widetilde{u}_i = \frac{1}{2}u_x(x_i)\Delta x_i + O(h^2), \qquad \widetilde{\widetilde{u}}_i = \frac{1}{2}u_x(x_i)\Delta x_i + O(h^2),$$

while

$$\Delta_+\bar{u}_i = \frac{1}{2}u_x(x_i)(\Delta x_i+\Delta x_{i+1})+O(h^2), \quad \Delta_-\bar{u}_i = \frac{1}{2}u_x(x_i)(\Delta x_i+\Delta x_{i-1})+O(h^2).$$

Clearly, when we are in a smooth and monotone region, namely when $u_x(x_i)$ is away from zero, the first argument in the minmod function (3.22) is of the same sign as the second and third arguments and is smaller in magnitude (for a uniform mesh it is about half of their magnitude), when h is small. Therefore, since the minmod function (3.23) picks the smallest argument (in magnitude) when all the arguments are of the same sign, the modified values $\widetilde{u}_i^{(\mathrm{mod})}$ and $\widetilde{\widetilde{u}}_i^{(\mathrm{mod})}$ in (3.22) will take the unmodified values $\widetilde{u}_i$ and $\widetilde{\widetilde{u}}_i$, respectively. That is, the limiter does not affect accuracy in smooth, monotone regions.

On the other hand, the TVD limiter (3.22) does kill accuracy at smooth extrema. This is demonstrated by numerical results and is a consequence of the general results about TVD schemes, that they are at most second-order accurate for smooth but non-monotone solutions [31]. Therefore, in practice we often use a total variation bounded (TVB) corrected limiter

$$\widetilde{m}(a_1, \cdots, a_\ell) = \begin{cases} a_1, & \text{if } |a_1| \le Mh^2, \\ m(a_1, \ldots, a_\ell), & \text{otherwise,} \end{cases}$$

instead of the original minmod function (3.23), where the TVB parameter M has to be chosen adequately [13]. The DG scheme would then be total variation bounded in the means (TVBM) and uniformly high-order accurate for smooth solutions. We will not discuss more details here and refer the readers to [13].

We would like to remark that the limiters discussed in this subsection were first used for finite-volume schemes [30]. When discussing limiters, the DG methods and finite-volume schemes have many similarities.

3.2.3 Error Estimates for Smooth Solutions

If we assume the exact solution of (3.7) is smooth, we can obtain optimal L^2-error estimates. Such error estimates can be obtained for the general nonlinear conservation law (3.7) and for fully discretized RKDG methods, see [58]. However, for simplicity we will give here the proof only for the semi-discrete DG scheme and the linear version of (3.7):

$$u_t + u_x = 0, \tag{3.32}$$

for which the monotone flux is taken as the simple upwind flux $\widehat{f}(u^-, u^+) = u^-$. Of course the proof is the same for $u_t + au_x = 0$ with any constant a.

Proposition 3.5. *The solution u_h of the* DG *scheme* (3.9) *for the* PDE (3.32) *with a smooth solution u satisfies the error estimate*

$$\|u - u_h\| \leq Ch^{k+1} \tag{3.33}$$

where C depends on u and its derivatives but is independent of h.

Proof. The DG scheme (3.9), when using the notation in (3.12), can be written as

$$B_i(u_h; v_h) = 0, \tag{3.34}$$

for all $v_h \in V_h$ and for all i. It is easy to verify that the exact solution of the PDE (3.32) also satisfies

$$B_i(u; v_h) = 0, \tag{3.35}$$

for all $v_h \in V_h$ and for all i. Subtracting (3.34) from (3.35) and using the linearity of B_i with respect to its first argument, we obtain the error equation

$$B_i(u - u_h; v_h) = 0, \tag{3.36}$$

for all $v_h \in V_h$ and for all i.

We now define a special projection P into V_h. For a given smooth function w, the projection Pw is the unique function in V_h which satisfies, for each i,

$$\int_{I_i} (Pw(x) - w(x))v_h(x)dx = 0 \qquad \forall v_h \in P^{k-1}(I_i); \qquad Pw(x^-_{i+\frac{1}{2}}) = w(x_{i+\frac{1}{2}}). \tag{3.37}$$

Standard approximation theory [7] implies, for a smooth function w,

$$\|Pw(x) - w(x)\| \leq Ch^{k+1} \tag{3.38}$$

where here and below C is a generic constant depending on w and its derivatives but independent of h (which may not have the same value in different places). In particular, in (3.38), $C = \widetilde{C}\|w\|_{H^{k+1}}$ where $\|w\|_{H^{k+1}}$ is the standard Sobolev $(k+1)$ norm and $\widetilde{C}$ is a constant independent of w.

We now take:

$$v_h = Pu - u_h \tag{3.39}$$

in the error equation (3.36), and denote

$$e_h = Pu - u_h, \qquad \varepsilon_h = u - Pu \tag{3.40}$$

to obtain

$$B_i(e_h; e_h) = -B_i(\varepsilon_h; e_h). \tag{3.41}$$

For the left-hand side of (3.41), we use the cell entropy inequality (see (3.14)) to obtain

$$B_i(e_h; e_h) = \frac{1}{2}\frac{d}{dt}\int_{I_i} (e_h)^2 dx + \widehat{F}_{i+\frac{1}{2}} - \widehat{F}_{i-\frac{1}{2}} + \Theta_{i-\frac{1}{2}}, \tag{3.42}$$

where $\Theta_{i-\frac{1}{2}} \geq 0$. As to the right-hand side of (3.41), we first write out all the terms

$$-B_i(\varepsilon_h; e_h) = -\int_{I_i} (\varepsilon_h)_t e_h dx + \int_{I_i} \varepsilon_h (e_h)_x dx - (\varepsilon_h)^-_{i+\frac{1}{2}} (e_h)^-_{i+\frac{1}{2}} + (\varepsilon_h)^-_{i-\frac{1}{2}} (e_h)^+_{i+\frac{1}{2}}.$$

Noticing the properties (3.37) of the projection P, we have

$$\int_{I_i} \varepsilon_h (e_h)_x dx = 0$$

because $(e_h)_x$ is a polynomial of degree at most $k-1$, and

$$(\varepsilon_h)^-_{i+\frac{1}{2}} = u_{i+\frac{1}{2}} - (Pu)^-_{i+\frac{1}{2}} = 0$$

for all i. Therefore, the right-hand side of (3.41) becomes

$$-B_i(\varepsilon_h; e_h) = -\int_{I_i} (\varepsilon_h)_t e_h dx \leq \frac{1}{2}\left(\int_{I_i} ((\varepsilon_h)_t)^2 dx + \int_{I_i} (e_h)^2 dx\right). \tag{3.43}$$

Plugging (3.42) and (3.43) into the equality (3.41), summing up over i, and using the approximation result (3.38), we obtain

$$\frac{d}{dt}\int_0^1 (e_h)^2 dx \leq \int_0^1 (e_h)^2 dx + Ch^{2k+2}.$$

A Gronwall's inequality, the fact that the initial error

$$\|u(\cdot, 0) - u_h(\cdot, 0)\| \leq Ch^{k+1}$$

(usually the initial condition $u_h(\cdot, 0)$ is taken as the L^2-projection of the analytical initial condition $u(\cdot, 0)$), and the approximation result (3.38) finally give us the error estimate (3.33). □

3.3 Comments for Multi-dimensional Cases

Even though we have only discussed the two-dimensional steady-state and one-dimensional time-dependent cases in previous subsections, most of the results also hold for multi-dimensional cases with arbitrary triangulations. For example, the semi-discrete DG method for the two-dimensional time-dependent conservation law

$$u_t + f(u)_x + g(u)_y = 0 \tag{3.44}$$

is defined as follows. The computational domain is partitioned into a collection of cells $\triangle_i$, which in 2D could be rectangles, triangles, etc., and the numerical solution is a polynomial of degree k in each cell $\triangle_i$. The degree k could change

with the cell, and there is no continuity requirement of the two polynomials along an interface of two cells. Thus, instead of only one degree of freedom per cell as in a finite-volume scheme, namely the cell average of the solution, there are now $K = \frac{(k+1)(k+2)}{2}$ degrees of freedom per cell for a DG method using piecewise k-th degree polynomials in 2D. These K degrees of freedom are chosen as the coefficients of the polynomial when expanded in a local basis. One could use a locally orthogonal basis to simplify the computation, but this is not essential.

The DG method is obtained by multiplying (3.44) by a test function $v(x, y)$ (which is also a polynomial of degree k in the cell), integrating over the cell $\triangle_j$, and integrating by parts:

$$\frac{d}{dt}\int_{\triangle_j} u(x,y,t)v(x,y)dxdy - \int_{\triangle_j} F(u)\cdot\nabla v\, dxdy + \int_{\partial\triangle_j} F(u)\cdot n\, v\, ds \;=\; 0, \quad (3.45)$$

where $F = (f, g)$, and n is the outward unit normal of the cell boundary $\partial\triangle_j$. The line integral in (3.45) is typically discretized by a Gaussian quadrature of sufficiently high order of accuracy,

$$\int_{\partial\triangle_j} F\cdot n\, v\, ds \;\approx\; |\partial\triangle_j| \sum_{k=1}^{q} \omega_k F(u(G_k,t))\cdot n\, v(G_k),$$

where $F(u(G_k, t)) \cdot n$ is replaced by a numerical flux (approximate or exact Riemann solvers). For scalar equations the numerical flux can be taken as any of the monotone fluxes discussed in Section 3.2 along the normal direction of the cell boundary. For example, one could use the simple Lax-Friedrichs flux, which is given by

$$F(u(G_k,t))\cdot n \approx \frac{1}{2}\left[\left(F(u^-(G_k,t)) + F(u^+(G_k,t))\right)\cdot n - \alpha\left(u^+(G_k,t) - u^-(G_k,t)\right)\right],$$

where α is taken as an upper bound for the eigenvalues of the Jacobian in the n direction, and u^- and u^+ are the values of u inside the cell $\triangle_j$ and outside the cell $\triangle_j$ (inside the neighboring cell) at the Gaussian point G_k. $v(G_k)$ is taken as $v^-(G_k)$, namely the value of v inside the cell $\triangle_j$ at the Gaussian point G_k. The volume integral term $\int_{\triangle_j} F(u)\cdot\nabla v\, dxdy$ can be computed either by a numerical quadrature or by a quadrature free implementation [2] for special systems such as the compressible Euler equations. Notice that if a locally orthogonal basis is chosen, the time derivative term $\frac{d}{dt}\int_{\triangle_j} u(x,y,t)v(x,y)dxdy$ would be explicit and there is no mass matrix to invert. However, even if the local basis is not orthogonal, one still only needs to invert a small $K \times K$ local mass matrix (by hand) and there is never a global mass matrix to invert as in a typical finite-element method.

For scalar equations (3.44), the cell entropy inequality described in Proposition 3.1 holds for arbitrary triangulation. The limiter described in Section 3.2.2 can also be defined for arbitrary triangulation, see [10]. Instead of the TVDM property given in Proposition 3.3, for multi-dimensional cases one can prove the

maximum norm stability of the limited scheme, see [10]. The optimal error estimate given in Proposition 3.5 can be proved for tensor product meshes and basis functions, and for certain specific triangulations when the usual piecewise k-th degree polynomial approximation spaces are used [39, 9]. For the most general cases, an L^2-error estimate of half an order lower $O(h^{k+\frac{1}{2}})$ can be proved [24], which is actually sharp [33].

For nonlinear hyperbolic equations including symmetrizable systems, if the solution of the PDE is smooth, L^2-error estimates of $O(h^{k+1/2} + \Delta t^2)$ where Δt is the time step can be obtained for the fully discrete Runge-Kutta discontinuous Galerkin method with second-order Runge-Kutta time discretization. For upwind fluxes the optimal $O(h^{k+1} + \Delta t^2)$ error estimate can be obtained. See [58, 59].

As an example of the excellent numerical performance of the RKDG scheme, we show in Figures 3.1 and 3.2 the solution of the second order (piecewise linear) and seventh order (piecewise polynomial of degree 6) DG methods for the linear transport equation

$$u_t + u_x = 0, \qquad \text{or} \qquad u_t + u_x + u_y = 0,$$

on the domain $(0, 2\pi) \times (0, T)$ or $(0, 2\pi)^2 \times (0, T)$ with the characteristic function of the interval $(\frac{\pi}{2}, \frac{3\pi}{2})$ or the square $(\frac{\pi}{2}, \frac{3\pi}{2})^2$ as initial condition and periodic boundary conditions [17]. Notice that the solution is for a *very long* time, $t = 100\pi$ (50 time periods), with a relatively coarse mesh. We can see that the second-order scheme smears the fronts, however the seventh-order scheme maintains the shape of the solution almost as well as the initial condition! The excellent performance can be achieved by the DG method on multi-dimensional linear systems using unstructured meshes, hence it is a very good method for solving, e.g. Maxwell equations of electromagnetism and linearized Euler equations of aeroacoustics.

To demonstrate that the DG method also works well for nonlinear systems, we show in Figure 3.3 the DG solution of the forward facing step problem by solving the compressible Euler equations of gas dynamics [15]. We can see that the roll-ups of the contact line caused by a physical instability are resolved well, especially by the third-order DG scheme.

In summary, we can say the following about the discontinuous Galerkin methods for conservation laws:

1. They can be used for arbitrary triangulation, including those with hanging nodes. Moreover, the degree of the polynomial, hence the order of accuracy, in each cell can be independently decided. Thus the method is ideally suited for *h-p* (mesh size and order of accuracy) refinements and adaptivity.
2. The methods have excellent parallel efficiency. Even with space time adaptivity and load balancing the parallel efficiency can still be over 80%, see [38].
3. They should be the methods of choice if geometry is complicated or if adaptivity is important, especially for problems with long time evolution of smooth solutions.

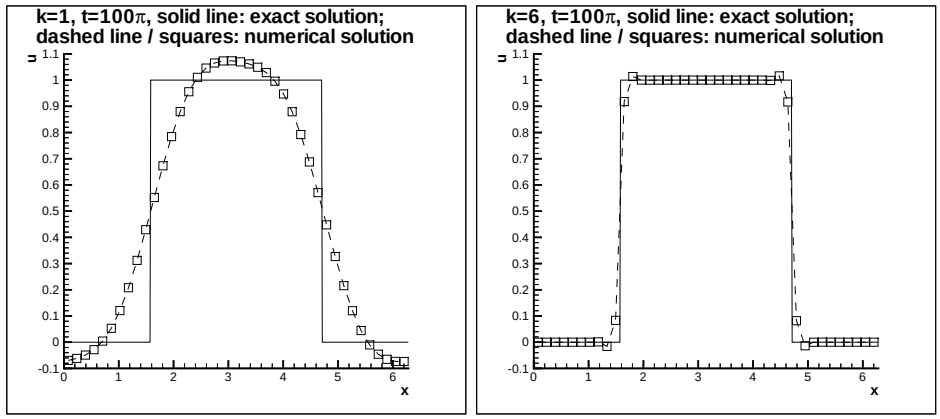

Figure 3.1: Transport equation: Comparison of the exact and the RKDG solutions at $T = 100\pi$ with second order (P^1, left) and seventh order (P^6, right) RKDG methods. One-dimensional results with 40 cells, exact solution (solid line) and numerical solution (dashed line and symbols, one point per cell).

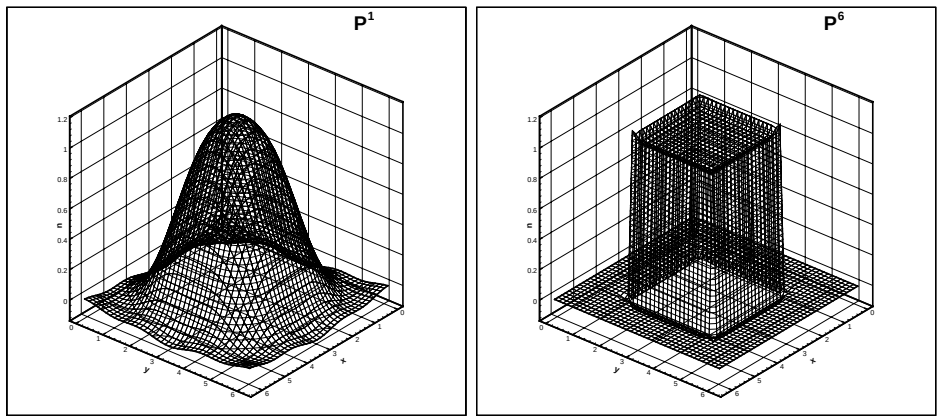

Figure 3.2: Transport equation: Comparison of the exact and the RKDG solutions at $T = 100\pi$ with second order (P^1, left) and seventh order (P^6, right) RKDG methods. Two-dimensional results with 40×40 cells.

4. For problems containing strong shocks, the nonlinear limiters are still less robust than the advanced WENO philosophy. There is a parameter (the TVB constant) for the user to tune for each problem, see [13, 10, 15]. For rectangular meshes the limiters work better than for triangular ones. In recent years, WENO based limiters have been investigated [35, 34, 36].

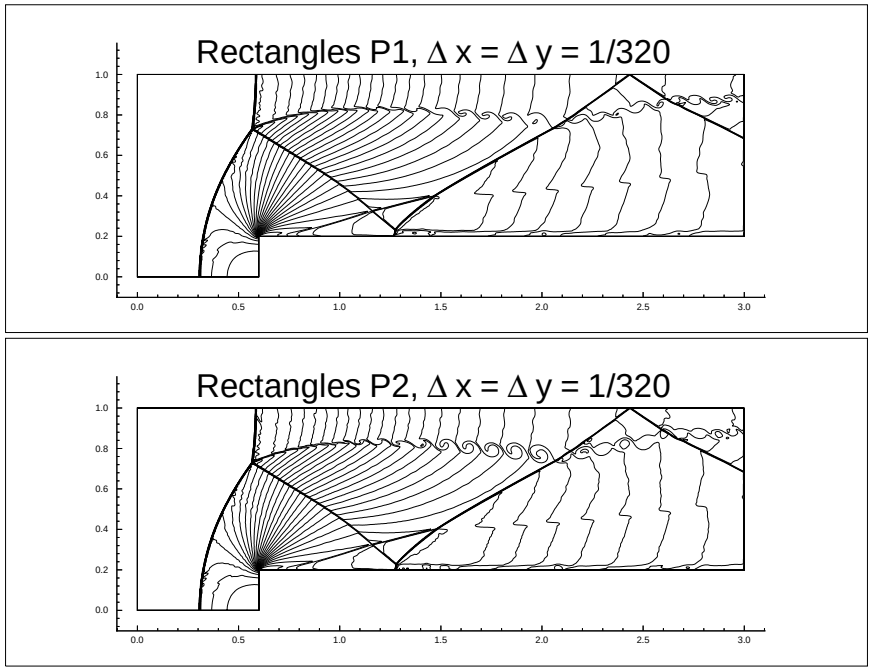

Figure 3.3: Forward facing step. Zoomed-in region. $\Delta x = \Delta y = \frac{1}{320}$. Top: P^1 elements; bottom: P^2 elements.

Chapter 4

Discontinuous Galerkin Method for Convection-Diffusion Equations

In this section we discuss the discontinuous Galerkin method for time-dependent convection-diffusion equations

$$u_t + \sum_{i=1}^{d} f_i(u)_{x_i} - \sum_{i=1}^{d}\sum_{j=1}^{d}(a_{ij}(u)u_{x_j})_{x_i} = 0, \tag{4.1}$$

where $(a_{ij}(u))$ is a symmetric, semi-positive definite matrix. There are several different formulations of discontinuous Galerkin methods for solving such equations, e.g., [1, 4, 6, 29, 45], however in this section we will only discuss the local discontinuous Galerkin (LDG) method [16].

For equations containing higher-order spatial derivatives, such as the convection-diffusion equation (4.1), discontinuous Galerkin methods cannot be directly applied. This is because the solution space, which consists of piecewise polynomials discontinuous at the element interfaces, is not regular enough to handle higher derivatives. This is a typical "non-conforming" case in finite elements. A naive and careless application of the discontinuous Galerkin method directly to the heat equation containing second derivatives could yield a method which behaves nicely in the computation but is "inconsistent" with the original equation and has $O(1)$ errors to the exact solution [17, 57].

The idea of local discontinuous Galerkin methods for time-dependent partial differential equations with higher derivatives, such as the convection-diffusion equation (4.1), is to rewrite the equation into a first-order system, then apply the discontinuous Galerkin method on the system. A key ingredient for the success of such methods is the correct design of interface numerical fluxes. These fluxes must

be designed to guarantee stability and local solvability of all the auxiliary variables introduced to approximate the derivatives of the solution. The local solvability of all the auxiliary variables is why the method is called a "local" discontinuous Galerkin method in [16].

The first local discontinuous Galerkin method was developed by Cockburn and Shu [16], for the convection-diffusion equation (4.1) containing second derivatives. Their work was motivated by the successful numerical experiments of Bassi and Rebay [3] for the compressible Navier-Stokes equations.

In the following we will discuss the stability and error estimates for the LDG method for convection-diffusion equations. We present details only for the one-dimensional case and will mention briefly the generalization to multi-dimensions in Section 4.4.

4.1 LDG Scheme Formulation

We consider the one-dimensional convection-diffusion equation

$$u_t + f(u)_x = (a(u)u_x)_x \tag{4.2}$$

with $a(u) \geq 0$. We rewrite this equation as the system

$$u_t + f(u)_x = (b(u)q)_x, \qquad q - B(u)_x = 0, \tag{4.3}$$

where

$$b(u) = \sqrt{a(u)}, \qquad B(u) = \int^u b(u)du. \tag{4.4}$$

The finite-element space is still given by (3.8). The semi-discrete LDG scheme is defined as follows. Find $u_h, q_h \in V_h^k$ such that, for all test functions $v_h, p_h \in V_h^k$ and all $1 \leq i \leq N$, we have

$$\begin{aligned} &\int_{I_i} (u_h)_t (v_h)dx - \int_{I_i} (f(u_h) - b(u_h)q_h)(v_h)_x dx \\ &\qquad + (\widehat{f} - \widehat{bq})_{i+\frac{1}{2}} (v_h)^-_{i+\frac{1}{2}} - (\widehat{f} - \widehat{bq})_{i-\frac{1}{2}} (v_h)^+_{i-\frac{1}{2}} = 0, \\ &\int_{I_i} q_h p_h dx + \int_{I_i} B(u_h)(p_h)_x dx - \widehat{B}_{i+\frac{1}{2}} (p_h)^-_{i+\frac{1}{2}} + \widehat{B}_{i-\frac{1}{2}} (p_h)^+_{i-\frac{1}{2}} = 0. \end{aligned} \tag{4.5}$$

Here, all the "hat" terms are the numerical fluxes, namely single-valued functions defined at the cell interfaces which typically depend on the discontinuous numerical solution from both sides of the interface. We already know from Section 3 that the convection flux $\widehat{f}$ should be chosen as a monotone flux. However, the upwinding principle is no longer a valid guiding principle for the design of the diffusion fluxes $\widehat{b}$, $\widehat{q}$ and $\widehat{B}$. In [16], sufficient conditions for the choices of these diffusion fluxes

to guarantee the stability of the scheme (4.5) are given. Here, we will discuss a particularly attractive choice, called "alternating fluxes", defined as

$$\widehat{b} = \frac{B(u_h^+) - B(u_h^-)}{u_h^+ - u_h^-}, \qquad \widehat{q} = q_h^+, \qquad \widehat{B} = B(u_h^-). \tag{4.6}$$

The important point is that $\widehat{q}$ and $\widehat{B}$ should be chosen from different directions. Thus, the choice

$$\widehat{b} = \frac{B(u_h^+) - B(u_h^-)}{u_h^+ - u_h^-}, \qquad \widehat{q} = q_h^-, \qquad \widehat{B} = B(u_h^+)$$

is also fine.

Notice that, from the second equation in the scheme (4.5), we can solve q_h explicitly and locally (in cell I_i) in terms of u_h, by inverting the small mass matrix inside the cell I_i. This is why the method is referred to as the "local" discontinuous Galerkin method.

4.2 Stability Analysis

Similar to the case for hyperbolic conservation laws, we have the following "cell entropy inequality" for the LDG method (4.5).

Proposition 4.1. *The solution u_h, q_h to the semi-discrete* LDG *scheme* (4.5) *satisfies the following "cell entropy inequality"*

$$\frac{1}{2}\frac{d}{dt}\int_{I_i} (u_h)^2\,dx + \int_{I_i} (q_h)^2 dx + \widehat{F}_{i+\frac{1}{2}} - \widehat{F}_{i-\frac{1}{2}} \le 0 \tag{4.7}$$

for some consistent entropy flux

$$\widehat{F}_{i+\frac{1}{2}} = \widehat{F}(u_h(x^-_{i+\frac{1}{2}}, t), q_h(x^-_{i+\frac{1}{2}}, t); u_h(x^+_{i+\frac{1}{2}}, t), q_h(x^+_{i+\frac{1}{2}}))$$

satisfying $\widehat{F}(u,u) = F(u) - ub(u)q$ where, as before, $F(u) = \int^u uf'(u)du$.

Proof. We introduce a short-hand notation

$$\begin{aligned} B_i(u_h, q_h; v_h, p_h) = &\int_{I_i} (u_h)_t (v_h) dx - \int_{I_i} (f(u_h) - b(u_h)q_h)(v_h)_x dx \\ &+ (\widehat{f} - \widehat{bq})_{i+\frac{1}{2}} (v_h)^-_{i+\frac{1}{2}} - (\widehat{f} - \widehat{bq})_{i-\frac{1}{2}} (v_h)^+_{i-\frac{1}{2}} \\ &+ \int_{I_i} q_h p_h dx + \int_{I_i} B(u_h)(p_h)_x dx - \widehat{B}_{i+\frac{1}{2}} (p_h)^-_{i+\frac{1}{2}} + \widehat{B}_{i-\frac{1}{2}} (p_h)^+_{i-\frac{1}{2}}. \end{aligned} \tag{4.8}$$

If we take $v_h = u_h$, $p_h = q_h$ in the scheme (4.5), we obtain

$$\begin{aligned} B_i(u_h, q_h; u_h, q_h) = &\int_{I_i} (u_h)_t (u_h) dx \qquad (4.9)\\ &- \int_{I_i} (f(u_h) - b(u_h)q_h)(u_h)_x dx \\ &+ (\widehat{f} - \widehat{bq})_{i+\frac{1}{2}} (u_h)^-_{i+\frac{1}{2}} - (\widehat{f} - \widehat{bq})_{i-\frac{1}{2}} (u_h)^+_{i-\frac{1}{2}} \qquad (4.10)\\ &+ \int_{I_i} (q_h)^2 dx + \int_{I_i} B(u_h)(q_h)_x dx - \widehat{B}_{i+\frac{1}{2}} (q_h)^-_{i+\frac{1}{2}} + \widehat{B}_{i-\frac{1}{2}} (q_h)^+_{i-\frac{1}{2}} \\ &= 0. \end{aligned}$$

If we denote $\widetilde{F}(u) = \int^u f(u)du$, then (4.9) becomes

$$\begin{aligned} B_i(u_h, q_h; u_h, q_h) = \frac{1}{2}\frac{d}{dt}\int_{I_i} (u_h)^2\, dx + \int_{I_i} (q_h)^2 dx \\ + \widehat{F}_{i+\frac{1}{2}} - \widehat{F}_{i-\frac{1}{2}} + \Theta_{i-\frac{1}{2}} = 0, \qquad (4.11) \end{aligned}$$

where

$$\widehat{F} = -\widetilde{F}(u_h^-) + \widehat{f} u_h^- - \widehat{b} q_h^+ u_h^- \qquad (4.12)$$

and

$$\Theta = -\widetilde{F}(u_h^-) + \widehat{f} u_h^- + \widetilde{F}(u_h^+) - \widehat{f} u_h^+, \qquad (4.13)$$

where we have used the definition of the numerical fluxes (4.6). Notice that we have omitted the subindex $i - \frac{1}{2}$ in the definitions of $\widehat{F}$ and Θ. It is easy to verify that the numerical entropy flux $\widehat{F}$ defined by (4.12) is consistent with the entropy flux $F(u) - ub(u)q$. As Θ in (4.13) is the same as that in (3.16) for the conservation law case, we readily have $\Theta \geq 0$. This finishes the proof of (4.7). □

We again note that the proof does not depend on the accuracy of the scheme, namely it holds for the piecewise polynomial space (3.8) with any degree k. Also, the same proof can be given for multi-dimensional LDG schemes on any triangulation.

As before, the cell entropy inequality trivially implies an L^2-stability of the numerical solution.

Proposition 4.2. *For periodic or compactly supported boundary conditions, the solution u_h, q_h to the semi-discrete* LDG *scheme* (4.5) *satisfies the following L^2-stability*

$$\frac{d}{dt}\int_0^1 (u_h)^2 dx + 2\int_0^1 (q_h)^2 dx \leq 0, \qquad (4.14)$$

or

$$\|u_h(\cdot, t)\| + 2\int_0^t \|q_h(\cdot, \tau)\| d\tau \leq \|u_h(\cdot, 0)\|. \qquad (4.15)$$

□

Notice that both the cell entropy inequality (4.7) and the L^2-stability (4.14) are valid regardless of whether the convection-diffusion equation (4.2) is convection-dominated or diffusion-dominated and regardless of whether the exact solution is smooth or not. The diffusion coefficient $a(u)$ can be degenerate (equal to zero) in any part of the domain. The LDG method is particularly attractive for convection-dominated convection-diffusion equations, when traditional continuous finite-element methods are less stable.

4.3 Error Estimates

Again, if we assume the exact solution of (4.2) is smooth, we can obtain optimal L^2-error estimates. Such error estimates can be obtained for the general nonlinear convection-diffusion equation (4.2), see [53]. However, for simplicity we will give here the proof only for the heat equation:

$$u_t = u_{xx} \tag{4.16}$$

defined on $[0, 1]$ with periodic boundary conditions.

Proposition 4.3. *The solution u_h and q_h to the semi-discrete* DG *scheme* (4.5) *for the* PDE (4.16) *with a smooth solution u satisfies the error estimate*

$$\int_0^1 \left(u(x,t) - u_h(x,t)\right)^2 dx + \int_0^t \int_0^1 \left(u_x(x,\tau) - q_h(x,\tau)\right)^2 dx d\tau \le C h^{2(k+1)}, \tag{4.17}$$

where C depends on u and its derivatives but is independent of h.

Proof. The DG scheme (4.5), when using the notation in (4.8), can be written as

$$B_i(u_h, q_h; v_h, p_h) = 0, \tag{4.18}$$

for all $v_h, p_h \in V_h$ and for all i. It is easy to verify that the exact solution u and $q = u_x$ of the PDE (4.16) also satisfies

$$B_i(u, q; v_h, p_h) = 0, \tag{4.19}$$

for all $v_h, p_h \in V_h$ and for all i. Subtracting (4.18) from (4.19) and using the linearity of B_i with respect to its first two arguments, we obtain the error equation

$$B_i(u - u_h, q - q_h; v_h, p_h) = 0, \tag{4.20}$$

for all $v_h, p_h \in V_h$ and for all i.

Recall the special projection P defined in (3.37). We also define another special projection Q as follows. For a given smooth function w, the projection Qw is the unique function in V_h which satisfies, for each i,

$$\int_{I_i} (Qw(x) - w(x)) v_h(x) dx = 0 \qquad \forall v_h \in P^{k-1}(I_i); \qquad Qw(x^+_{i-\frac{1}{2}}) = w(x_{i-\frac{1}{2}}). \tag{4.21}$$

Similar to P, we also have, by standard approximation theory [7], that

$$\|Qw(x) - w(x)\| \le Ch^{k+1}, \qquad \forall w \in H^{k+1}(\Omega), \tag{4.22}$$

where C is a constant depending on w and its derivatives but independent of h.

We now take

$$v_h = Pu - u_h, \qquad p_h = Qq - q_h \tag{4.23}$$

in the error equation (4.20), and denote

$$e_h = Pu - u_h, \;\; \bar{e}_h = Qq - q_h; \qquad \varepsilon_h = u - Pu, \;\; \bar{\varepsilon}_h = q - Qq, \tag{4.24}$$

to obtain

$$B_i(e_h, \bar{e}_h; e_h, \bar{e}_h) = -B_i(\varepsilon_h, \bar{\varepsilon}_h; e_h, \bar{e}_h). \tag{4.25}$$

For the left-hand side of (4.25), we use the cell entropy inequality (see (4.11)) to obtain

$$B_i(e_h, \bar{e}_h; e_h, \bar{e}_h) = \frac{1}{2}\frac{d}{dt}\int_{I_i} (e_h)^2 dx + \int_{I_i} (\bar{e}_h)^2 dx + \widehat{F}_{i+\frac{1}{2}} - \widehat{F}_{i-\frac{1}{2}} + \Theta_{i-\frac{1}{2}}, \tag{4.26}$$

where $\Theta_{i-\frac{1}{2}} \ge 0$ (in fact we can easily verify, from (4.13), that $\Theta_{i-\frac{1}{2}} = 0$ for the special case of the heat equation (4.16)). As to the right-hand side of (4.25), we first write out all the terms

$$\begin{aligned} -B_i(\varepsilon_h, \bar{\varepsilon}_h; e_h, \bar{e}_h) = &- \int_{I_i} (\varepsilon_h)_t e_h dx \\ &- \int_{I_i} \bar{\varepsilon}_h (e_h)_x dx + (\bar{\varepsilon}_h)^+_{i+\frac{1}{2}} (e_h)^-_{i+\frac{1}{2}} - (\bar{\varepsilon}_h)^+_{i-\frac{1}{2}} (e_h)^+_{i-\frac{1}{2}} \\ &- \int_{I_i} \bar{\varepsilon}_h \bar{e}_h dx \\ &- \int_{I_i} \varepsilon_h (\bar{e}_h)_x dx + (\varepsilon_h)^-_{i+\frac{1}{2}} (\bar{e}_h)^-_{i+\frac{1}{2}} - (\varepsilon_h)^-_{i-\frac{1}{2}} (\bar{e}_h)^+_{i-\frac{1}{2}}. \end{aligned}$$

Noticing the properties (3.37) and (4.21) of the projections P and Q, we have

$$\int_{I_i} \bar{\varepsilon}_h (e_h)_x dx = 0, \qquad \int_{I_i} \varepsilon_h (\bar{e}_h)_x dx = 0,$$

because $(e_h)_x$ and $(\bar{e}_h)_x$ are polynomials of degree at most $k-1$, and

$$(\varepsilon_h)^-_{i+\frac{1}{2}} = u_{i+\frac{1}{2}} - (Pu)^-_{i+\frac{1}{2}} = 0, \qquad (\bar{\varepsilon}_h)^+_{i+\frac{1}{2}} = q_{i+\frac{1}{2}} - (Qq)^+_{i+\frac{1}{2}} = 0,$$

for all i. Therefore, the right-hand side of (4.25) becomes

$$\begin{aligned} -B_i(\varepsilon_h, \bar{\varepsilon}_h; e_h, \bar{e}_h) &= -\int_{I_i} (\varepsilon_h)_t e_h dx - \int_{I_i} \bar{\varepsilon}_h \bar{e}_h dx \\ &\le \frac{1}{2}\left(\int_{I_i} ((\varepsilon_h)_t)^2 dx + \int_{I_i} (e_h)^2 dx + \int_{I_i} (\bar{\varepsilon}_h)^2 dx + \int_{I_i} (\bar{e}_h)^2 dx \right). \end{aligned} \tag{4.27}$$

Plugging (4.26) and (4.27) into the equality (4.25), summing up over i, and using the approximation results (3.38) and (4.22), we obtain

$$\frac{d}{dt}\int_0^1 (e_h)^2 dx + \int_0^1 (\bar{e}_h)^2 dx \leq \int_0^1 (e_h)^2 dx + Ch^{2k+2}.$$

A Gronwall's inequality, the fact that the initial error

$$\|u(\cdot,0) - u_h(\cdot,0)\| \leq Ch^{k+1}$$

and the approximation results (3.38) and (4.22) finally give us the error estimate (4.17). □

4.4 Multi-Dimensions

Even though we have only discussed one-dimensional cases in this section, the algorithm and its analysis can be easily generalized to the multi-dimensional equation (4.1). The stability analysis is the same as for the one-dimensional case in Section 4.2. The optimal $O(h^{k+1})$ error estimates can be obtained on tensor product meshes and polynomial spaces, along the same line as that in Section 4.3. For general triangulations and piecewise polynomials of degree k, a sub-optimal error estimate of $O(h^k)$ can be obtained. We will not provide the details here and refer to [16, 53].

Chapter 5

Discontinuous Galerkin Method for PDEs Containing Higher-Order Spatial Derivatives

We now consider the DG method for solving PDEs containing higher-order spatial derivatives. Even though there are other possible DG schemes for such PDEs, e.g. those designed in [6], we will only discuss the local discontinuous Galerkin (LDG) method in this section.

5.1 LDG Scheme for the KdV Equations

We first consider PDEs containing third spatial derivatives. These are usually nonlinear dispersive wave equations, for example the following general KdV-type equations

$$u_t + \sum_{i=1}^{d} f_i(u)_{x_i} + \sum_{i=1}^{d} \Big(r_i'(u) \sum_{j=1}^{d} g_{ij}(r_i(u)_{x_i})_{x_j} \Big)_{x_i} = 0, \tag{5.1}$$

where $f_i(u)$, $r_i(u)$ and $g_{ij}(q)$ are arbitrary (smooth) nonlinear functions. The one-dimensional KdV equation

$$u_t + (\alpha u + \beta u^2)_x + \sigma u_{xxx} = 0, \tag{5.2}$$

where α, β and σ are constants, is a special case of the general class (5.1).

Stable LDG schemes for solving (5.1) were first designed in [55]. We will concentrate our discussion on the one-dimensional case. For the one-dimensional generalized KdV-type equations

$$u_t + f(u)_x + (r'(u)g(r(u)_x)_x)_x = 0, \tag{5.3}$$

where $f(u)$, $r(u)$ and $g(q)$ are arbitrary (smooth) nonlinear functions, the LDG method is based on rewriting it as the following system,

$$u_t + (f(u) + r'(u)p)_x = 0, \qquad p - g(q)_x = 0, \qquad q - r(u)_x = 0. \tag{5.4}$$

The finite-element space is still given by (3.8). The semi-discrete LDG scheme is defined as follows. Find $u_h, p_h, q_h \in V_h^k$ such that, for all test functions $v_h, w_h, z_h \in V_h^k$ and all $1 \le i \le N$, we have

$$\begin{aligned}
&\int_{I_i} (u_h)_t (v_h) dx - \int_{I_i} (f(u_h) + r'(u_h)p_h)(v_h)_x dx \\
&\quad + (\widehat{f} + \widehat{r'}\widehat{p})_{i+\frac{1}{2}} (v_h)^-_{i+\frac{1}{2}} - (\widehat{f} + \widehat{r'}\widehat{p})_{i-\frac{1}{2}} (v_h)^+_{i-\frac{1}{2}} = 0, \\
&\int_{I_i} p_h w_h dx + \int_{I_i} g(q_h)(w_h)_x dx - \widehat{g}_{i+\frac{1}{2}} (w_h)^-_{i+\frac{1}{2}} + \widehat{g}_{i-\frac{1}{2}} (w_h)^+_{i-\frac{1}{2}} = 0, \\
&\int_{I_i} q_h z_h dx + \int_{I_i} r(u_h)(z_h)_x dx - \widehat{r}_{i+\frac{1}{2}} (z_h)^-_{i+\frac{1}{2}} + \widehat{r}_{i-\frac{1}{2}} (z_h)^+_{i-\frac{1}{2}} = 0.
\end{aligned} \tag{5.5}$$

Here again, all the "hat" terms are the numerical fluxes, namely single-valued functions defined at the cell interfaces which typically depend on the discontinuous numerical solution from both sides of the interface. We already know from Section 3 that the convection flux $\widehat{f}$ should be chosen as a monotone flux. It is important to design the other fluxes suitably in order to guarantee stability of the resulting LDG scheme. In fact, the upwinding principle is still a valid guiding principle here, since the KdV-type equation (5.3) is a dispersive wave equation for which waves are propagating with a direction. For example, the simple linear equation

$$u_t + u_{xxx} = 0,$$

which corresponds to (5.3) with $f(u) = 0$, $r(u) = u$ and $g(q) = q$, admits the following simple wave solution

$$u(x,t) = \sin(x+t),$$

that is, information propagates from right to left. This motivates the following choice of numerical fluxes, discovered in [55]:

$$\widehat{r'} = \frac{r(u_h^+) - r(u_h^-)}{u_h^+ - u_h^-}, \qquad \widehat{p} = p_h^+, \qquad \widehat{g} = \widehat{g}(q_h^-, q_h^+), \qquad \widehat{r} = r(u_h^-). \tag{5.6}$$

Here, $-\widehat{g}(q_h^-, q_h^+)$ is a monotone flux for $-g(q)$, namely $\widehat{g}$ is a non-increasing function in the first argument and a non-decreasing function in the second argument. The important point is again the "alternating fluxes", namely $\widehat{p}$ and $\widehat{r}$ should come from opposite sides. Thus

$$\widehat{r'} = \frac{r(u_h^+) - r(u_h^-)}{u_h^+ - u_h^-}, \qquad \widehat{p} = p_h^-, \qquad \widehat{g} = \widehat{g}(q_h^-, q_h^+), \qquad \widehat{r} = r(u_h^+)$$

would also work.

Notice that, from the third equation in the scheme (5.5), we can solve q_h explicitly and locally (in cell I_i) in terms of u_h, by inverting the small mass matrix inside the cell I_i. Then, from the second equation in the scheme (5.5), we can solve p_h explicitly and locally (in cell I_i) in terms of q_h. Thus only u_h is the global unknown and the auxiliary variables q_h and p_h can be solved in terms of u_h locally. This is why the method is referred to as the "local" discontinuous Galerkin method.

5.1.1 Stability Analysis

Similar to the case for hyperbolic conservation laws and convection-diffusion equations, we have the following "cell entropy inequality" for the LDG method (5.5).

Proposition 5.1. *The solution u_h to the semi-discrete* LDG *scheme* (5.5) *satisfies the following "cell entropy inequality"*

$$\frac{1}{2}\frac{d}{dt}\int_{I_i} (u_h)^2\, dx + \widehat{F}_{i+\frac{1}{2}} - \widehat{F}_{i-\frac{1}{2}} \le 0 \tag{5.7}$$

for some consistent entropy flux

$$\widehat{F}_{i+\frac{1}{2}} = \widehat{F}(u_h(x_{i+\frac{1}{2}}^-, t), p_h(x_{i+\frac{1}{2}}^-, t), q_h(x_{i+\frac{1}{2}}^-, t); u_h(x_{i+\frac{1}{2}}^+, t), p_h(x_{i+\frac{1}{2}}^+, t), q_h(x_{i+\frac{1}{2}}^+))$$

satisfying $\widehat{F}(u,u) = F(u) + ur'(u)p - G(q)$ where $F(u) = \int^u uf'(u)du$ and $G(q) = \int^q qg(q)dq$.

Proof. We introduce a short-hand notation

$$\begin{aligned} B_i(u_h,p_h,q_h;v_h,w_h,z_h) &= \int_{I_i}(u_h)_t(v_h)dx - \int_{I_i}(f(u_h)+r'(u_h)p_h)(v_h)_x dx \\ &+ (\widehat{f}+\widehat{r'}\widehat{p})_{i+\frac{1}{2}}(v_h)^-_{i+\frac{1}{2}} - (\widehat{f}+\widehat{r'}\widehat{p})_{i-\frac{1}{2}}(v_h)^+_{i-\frac{1}{2}} \\ &+ \int_{I_i} p_h w_h dx \\ &+ \int_{I_i} g(q_h)(w_h)_x dx - \widehat{g}_{i+\frac{1}{2}}(w_h)^-_{i+\frac{1}{2}} + \widehat{g}_{i-\frac{1}{2}}(w_h)^+_{i-\frac{1}{2}} \\ &+ \int_{I_i} q_h z_h dx \\ &+ \int_{I_i} r(u_h)(z_h)_x dx - \widehat{r}_{i+\frac{1}{2}}(z_h)^-_{i+\frac{1}{2}} + \widehat{r}_{i-\frac{1}{2}}(z_h)^+_{i-\frac{1}{2}}. \end{aligned} \tag{5.8}$$

If we take $v_h = u_h$, $w_h = q_h$ and $z_h = -p_h$ in the scheme (5.5), we obtain

$$\begin{aligned} B_i(u_h,p_h,q_h;u_h,q_h,-p_h) &= \int_{I_i}(u_h)_t(u_h)dx \\ &- \int_{I_i}(f(u_h)+r'(u_h)p_h)(u_h)_x dx \\ &+ (\widehat{f}+\widehat{r'}\widehat{p})_{i+\frac{1}{2}}(u_h)^-_{i+\frac{1}{2}} \\ &- (\widehat{f}+\widehat{r'}\widehat{p})_{i-\frac{1}{2}}(u_h)^+_{i-\frac{1}{2}} \\ &+ \int_{I_i} p_h q_h dx \\ &+ \int_{I_i} g(q_h)(q_h)_x dx - \widehat{g}_{i+\frac{1}{2}}(q_h)^-_{i+\frac{1}{2}} + \widehat{g}_{i-\frac{1}{2}}(q_h)^+_{i-\frac{1}{2}} \\ &- \int_{I_i} q_h p_h dx \\ &- \int_{I_i} r(u_h)(p_h)_x dx + \widehat{r}_{i+\frac{1}{2}}(p_h)^-_{i+\frac{1}{2}} - \widehat{r}_{i-\frac{1}{2}}(p_h)^+_{i-\frac{1}{2}} \\ &= 0. \end{aligned} \tag{5.9}$$

If we denote $\widetilde{F}(u) = \int^u f(u)du$ and $\widetilde{G}(q) = \int^q g(q)dq$, then (5.9) becomes

$$B_i(u_h,p_h,q_h;u_h,q_h,-p_h) = \frac{1}{2}\frac{d}{dt}\int_{I_i}(u_h)^2\,dx + \widehat{F}_{i+\frac{1}{2}} - \widehat{F}_{i-\frac{1}{2}} + \Theta_{i-\frac{1}{2}} = 0, \tag{5.10}$$

where

$$\widehat{F} = -\widetilde{F}(u_h^-) + \widehat{f}u_h^- + \widetilde{G}(q_h^-) + \widehat{r'}p_h^+u_h^- - \widehat{g}q_h^-, \tag{5.11}$$

and

$$\Theta = \left(-\widetilde{F}(u_h^-) + \widehat{f}u_h^- + \widetilde{F}(u_h^+) - \widehat{f}u_h^+\right) + \left(\widetilde{G}(q_h^-) - \widehat{g}q_h^- - \widetilde{G}(q_h^+) + \widehat{g}q_h^+\right), \quad (5.12)$$

where we have used the definition of the numerical fluxes (5.6). Notice that we have omitted the subindex $i - \frac{1}{2}$ in the definitions of $\widehat{F}$ and Θ. It is easy to verify that the numerical entropy flux $\widehat{F}$ defined by (5.11) is consistent with the entropy flux $F(u) + ur'(u)p - G(q)$. The terms inside the first parenthesis for Θ in (5.12) are the same as that in (3.16) for the conservation law case; those inside the second parenthesis are the same as those inside the first parenthesis, if we replace q_h by u_h, $-\widetilde{G}$ by $\widetilde{F}$, and $-\widehat{g}$ by $\widehat{f}$ (recall that $-\widehat{g}$ is a monotone flux). We therefore readily have $\Theta \geq 0$. This finishes the proof of (5.7). □

We observe once more that the proof does not depend on the accuracy of the scheme, namely it holds for the piecewise polynomial space (3.8) with any degree k. Also, the same proof can be given for the multi-dimensional LDG scheme solving (5.1) on any triangulation.

As before, the cell entropy inequality trivially implies an L^2-stability of the numerical solution.

Proposition 5.2. *For periodic or compactly supported boundary conditions, the solution u_h to the semi-discrete* LDG *scheme* (5.5) *satisfies the L^2-stability*

$$\frac{d}{dt}\int_0^1 (u_h)^2 dx \leq 0, \quad (5.13)$$

or

$$\|u_h(\cdot, t)\| \leq \|u_h(\cdot, 0)\|. \quad (5.14)$$

□

Again, both the cell entropy inequality (5.7) and the L^2-stability (5.13) are valid regardless of whether the KdV-type equation (5.3) is convection-dominated or dispersion-dominated and regardless of whether the exact solution is smooth or not. The dispersion flux $r'(u)g(r(u)_x)_x$ can be degenerate (equal to zero) in any part of the domain. The LDG method is particularly attractive for convection-dominated convection-dispersion equations, when traditional continuous finite-element methods may be less stable. In [55], this LDG method is used to study the dispersion limit of the Burgers equation, for which the third derivative dispersion term in (5.3) has a small coefficient which tends to zero.

5.1.2 Error Estimates

For error estimates we once again assume the exact solution of (5.3) is smooth. The error estimates can be obtained for a general class of nonlinear convection-dispersion equations which is a subclass of (5.3), see [53]. However, for simplicity we will give here only the proof for the linear equation

$$u_t + u_x + u_{xxx} = 0 \quad (5.15)$$

defined on $[0,1]$ with periodic boundary conditions.

Proposition 5.3. *The solution u_h to the semi-discrete* LDG *scheme* (5.5) *for the* PDE (5.15) *with a smooth solution u satisfies the following error estimate*

$$\|u - u_h\| \le Ch^{k+\frac{1}{2}}, \tag{5.16}$$

where C depends on u and its derivatives but is independent of h.

Proof. The LDG scheme (5.5), when using the notation in (5.8), can be written as

$$B_i(u_h, p_h, q_h; v_h, w_h, z_h) = 0, \tag{5.17}$$

for all $v_h, w_h, z_h \in V_h$ and for all i. It is easy to verify that the exact solution u, $q = u_x$ and $p = u_{xx}$ of the PDE (5.15) also satisfies

$$B_i(u, p, q; v_h, w_h, z_h) = 0, \tag{5.18}$$

for all $v_h, w_h, z_h \in V_h$ and for all i. Subtracting (5.17) from (5.18) and using the linearity of B_i with respect to its first three arguments, we obtain the error equation

$$B_i(u - u_h, p - p_h, q - q_h; v_h, w_h, z_h) = 0, \tag{5.19}$$

for all $v_h, w_h, z_h \in V_h$ and for all i.

Recall the special projection P defined in (3.37). We also denote the standard L^2-projection as R: for a given smooth function w, the projection Rw is the unique function in V_h which satisfies, for each i,

$$\int_{I_i} (Rw(x) - w(x))v_h(x)dx = 0 \qquad \forall v_h \in P^k(I_i). \tag{5.20}$$

Similar to P, we also have, by the standard approximation theory [7], that

$$\|Rw(x) - w(x)\| + \sqrt{h}\|Rw(x) - w(x)\|_\Gamma \le Ch^{k+1} \tag{5.21}$$

for a smooth function w, where C is a constant depending on w and its derivatives but independent of h, and $\|v\|_\Gamma$ is the usual L^2-norm on the cell interfaces of the mesh, which for this one-dimensional case is

$$\|v\|_\Gamma^2 = \sum_i \left((v_{i+\frac{1}{2}}^-)^2 + (v_{i-\frac{1}{2}}^+)^2 \right).$$

We now take

$$v_h = Pu - u_h, \qquad w_h = Rq - q_h, \qquad z_h = p_h - Rp \tag{5.22}$$

in the error equation (5.19), and denote

$$\begin{aligned} &e_h = Pu - u_h, \ \ \bar{e}_h = Rq - q_h, \\ &\bar{\bar{e}}_h = Rp - p_h; \quad \varepsilon_h = u - Pu, \ \ \bar{\varepsilon}_h = q - Rq, \ \ \bar{\bar{\varepsilon}}_h = p - Rp, \end{aligned} \tag{5.23}$$

to obtain

$$B_i(e_h, \bar{\bar{e}}_h, \bar{e}_h, ; e_h, \bar{e}_h, -\bar{\bar{e}}_h) = -B_i(\varepsilon_h, \bar{\bar{\varepsilon}}_h, \bar{\varepsilon}_h; e_h, \bar{e}_h, -\bar{\bar{e}}_h). \tag{5.24}$$

For the left-hand side of (5.24), we use the cell entropy inequality (see (5.10)) to obtain

$$B_i(e_h, \bar{\bar{e}}_h, \bar{e}_h, ; e_h, \bar{e}_h, -\bar{\bar{e}}_h) = \frac{1}{2}\frac{d}{dt}\int_{I_i} (e_h)^2 dx + \widehat{F}_{i+\frac{1}{2}} - \widehat{F}_{i-\frac{1}{2}} + \Theta_{i-\frac{1}{2}} \tag{5.25}$$

where we can easily verify, based on the formula (5.12) and for the PDE (5.15), that

$$\Theta_{i-\frac{1}{2}} = \frac{1}{2}\left((e_h)^+_{i-\frac{1}{2}} - (e_h)^-_{i-\frac{1}{2}}\right)^2 + \frac{1}{2}\left((\bar{e}_h)^+_{i-\frac{1}{2}} - (\bar{e}_h)^-_{i-\frac{1}{2}}\right)^2. \tag{5.26}$$

As to the right-hand side of (5.24), we first write out all the terms

$$\begin{aligned}
&-B_i(\varepsilon_h, \bar{\bar{\varepsilon}}_h, \bar{\varepsilon}_h; e_h, \bar{e}_h, -\bar{\bar{e}}_h) \\
&\quad = -\int_{I_i} (\varepsilon_h)_t e_h dx \\
&\quad + \int_{I_i} (\varepsilon_h + \bar{\bar{\varepsilon}}_h)(e_h)_x dx - (\varepsilon_h^- + \bar{\bar{\varepsilon}}_h^+)_{i+\frac{1}{2}}(e_h)^-_{i+\frac{1}{2}} + (\varepsilon_h^- + \bar{\bar{\varepsilon}}_h^+)_{i-\frac{1}{2}}(e_h)^+_{i-\frac{1}{2}} \\
&\quad - \int_{I_i} \bar{\bar{\varepsilon}}_h \bar{e}_h dx - \int_{I_i} \bar{\varepsilon}_h (\bar{e}_h)_x dx + (\bar{\varepsilon}_h)^+_{i+\frac{1}{2}}(\bar{e}_h)^-_{i+\frac{1}{2}} - (\bar{\varepsilon}_h)^+_{i-\frac{1}{2}}(\bar{e}_h)^+_{i-\frac{1}{2}} \\
&\quad + \int_{I_i} \bar{\varepsilon}_h \bar{\bar{e}}_h dx + \int_{I_i} \varepsilon_h (\bar{\bar{e}}_h)_x dx - (\varepsilon_h)^-_{i+\frac{1}{2}}(\bar{\bar{e}}_h)^-_{i+\frac{1}{2}} + (\varepsilon_h)^-_{i-\frac{1}{2}}(\bar{\bar{e}}_h)^+_{i-\frac{1}{2}}.
\end{aligned}$$

Noticing the properties (3.37) and (5.20) of the projections P and R, we have

$$\int_{I_i} (\varepsilon_h + \bar{\bar{\varepsilon}}_h)(e_h)_x dx = 0, \qquad \int_{I_i} \bar{\bar{\varepsilon}}_h \bar{e}_h dx = 0, \qquad \int_{I_i} \bar{\varepsilon}_h (\bar{e}_h)_x dx = 0,$$

$$\int_{I_i} \bar{\varepsilon}_h \bar{\bar{e}}_h dx = 0, \qquad \int_{I_i} \varepsilon_h (\bar{\bar{e}}_h)_x dx = 0,$$

because $(e_h)_x$, $(\bar{e}_h)_x$ and $(\bar{\bar{e}}_h)_x$ are polynomials of degree at most $k-1$, and $\bar{e}_h$ and $\bar{\bar{e}}_h$ are polynomials of degree at most k. Also,

$$(\varepsilon_h)^-_{i+\frac{1}{2}} = u_{i+\frac{1}{2}} - (Pu)^-_{i+\frac{1}{2}} = 0$$

for all i. Therefore, the right-hand side of (5.24) becomes

$$\begin{aligned}
&-B_i(\varepsilon_h, \bar{\bar{\varepsilon}}_h, \bar{\varepsilon}_h; e_h, \bar{e}_h, -\bar{\bar{e}}_h) \\
&\quad = -\int_{I_i} (\varepsilon_h)_t e_h dx - (\bar{\bar{\varepsilon}}_h)^+_{i+\frac{1}{2}}(e_h)^-_{i+\frac{1}{2}} + (\bar{\bar{\varepsilon}}_h)^+_{i-\frac{1}{2}}(e_h)^+_{i-\frac{1}{2}} \\
&\qquad\qquad + (\bar{\varepsilon}_h)^+_{i+\frac{1}{2}}(\bar{e}_h)^-_{i+\frac{1}{2}} - (\bar{\varepsilon}_h)^+_{i-\frac{1}{2}}(\bar{e}_h)^+_{i-\frac{1}{2}}
\end{aligned}$$

$$
\begin{aligned}
&= -\int_{I_i} (\varepsilon_h)_t e_h dx + \widehat{H}_{i+\frac{1}{2}} - \widehat{H}_{i-\frac{1}{2}} \\
&\quad + (\bar{\bar{\varepsilon}}_h)^+_{i-\frac{1}{2}} \left((e_h)^+_{i-\frac{1}{2}} - (e_h)^-_{i-\frac{1}{2}} \right) - (\bar{\varepsilon}_h)^+_{i-\frac{1}{2}} \left((\bar{e}_h)^+_{i-\frac{1}{2}} - (\bar{e}_h)^-_{i-\frac{1}{2}} \right) \qquad (5.27) \\
&\leq \widehat{H}_{i+\frac{1}{2}} - \widehat{H}_{i-\frac{1}{2}} + \frac{1}{2} \left[\int_{I_i} ((\varepsilon_h)_t)^2 dx + \int_{I_i} (e_h)^2 dx \right. \\
&\qquad\qquad + \left((\bar{\bar{\varepsilon}}_h)^+_{i-\frac{1}{2}} \right)^2 + \left((e_h)^+_{i-\frac{1}{2}} - (e_h)^-_{i-\frac{1}{2}} \right)^2 \\
&\qquad\qquad \left. + \left((\bar{\varepsilon}_h)^+_{i-\frac{1}{2}} \right)^2 + \left((\bar{e}_h)^+_{i-\frac{1}{2}} - (\bar{e}_h)^-_{i-\frac{1}{2}} \right)^2 \right].
\end{aligned}
$$

Plugging (5.25), (5.26) and (5.27) into the equality (5.24), summing up over i, and using the approximation results (3.38) and (5.21), we obtain

$$\frac{d}{dt} \int_0^1 (e_h)^2 dx \leq \int_0^1 (e_h)^2 dx + Ch^{2k+1}.$$

A Gronwall's inequality, the fact that the initial error

$$\|u(\cdot, 0) - u_h(\cdot, 0)\| \leq Ch^{k+1},$$

and the approximation results (3.38) and (5.21) finally give us the error estimate (5.16). □

We note that the error estimate (5.16) is half an order lower than optimal. Technically, this is because we are unable to use the special projections as before to eliminate the interface terms involving $\bar{\varepsilon}_h$ and $\bar{\bar{\varepsilon}}_h$ in (5.27). Numerical experiments in [55] indicate that both the L^2- and L^∞-errors are of the optimal $(k+1)$-th order of accuracy.

5.2 LDG Schemes for Other Higher-Order PDEs

In this subsection we list some of the higher-order PDEs for which stable DG methods have been designed in the literature. We will concentrate on the discussion of LDG schemes.

5.2.1 Bi-harmonic Equations

An LDG scheme for solving the time-dependent convection-bi-harmonic equation

$$u_t + \sum_{i=1}^{d} f_i(u)_{x_i} + \sum_{i=1}^{d} (a_i(u_{x_i}) u_{x_i x_i})_{x_i x_i} = 0, \qquad (5.28)$$

where $f_i(u)$ and $a_i(q) \geq 0$ are arbitrary functions, was designed in [56]. The numerical fluxes are chosen following the same "alternating fluxes" principle similar to the second-order convection-diffusion equation (4.1), see (4.6). A cell entropy inequality and the L^2-stability of the LDG scheme for the nonlinear equation (5.28) can be proved [56], which do not depend on the smoothness of the solution of (5.28), the order of accuracy of the scheme, or the triangulation.

5.2.2 Fifth-Order Convection-Dispersion Equations

An LDG scheme for solving the following fifth-order convection-dispersion equation

$$u_t + \sum_{i=1}^{d} f_i(u)_{x_i} + \sum_{i=1}^{d} g_i(u_{x_i x_i})_{x_i x_i x_i} = 0, \tag{5.29}$$

where $f_i(u)$ and $g_i(q)$ are arbitrary functions, was designed in [56]. The numerical fluxes are chosen following the same upwinding and "alternating fluxes" principle similar to the third-order KdV-type equations (5.1), see (5.6). A cell entropy inequality and the L^2-stability of the LDG scheme for the nonlinear equation (5.29) can be proved [56], which again do not depend on the smoothness of the solution of (5.29), the order of accuracy of the scheme, or the triangulation.

Stable LDG schemes for similar equations with sixth or higher derivatives can also be designed along similar lines.

5.2.3 The $K(m, n)$ Equations

LDG methods for solving the $K(m, n)$ equations

$$u_t + (u^m)_x + (u^n)_{xxx} = 0, \tag{5.30}$$

where m and n are positive integers, have been designed in [27]. These $K(m, n)$ equations were introduced by Rosenau and Hyman in [40] to study the so-called *compactons*, namely the compactly supported solitary waves solutions. For the special case of $m = n$ being an odd positive integer, LDG schemes which are stable in the L^{m+1}-norm can be designed (see [27]). For other cases, we can also design LDG schemes based on a linearized stability analysis, which perform well in numerical simulation for the fully nonlinear equation (5.30).

5.2.4 The KdV-Burgers-Type (KdVB) Equations

LDG methods for solving the KdV-Burgers-type (KdVB) equations

$$u_t + f(u)_x - (a(u)u_x)_x + (r'(u)g(r(u)_x)_x)_x = 0, \tag{5.31}$$

where $f(u)$, $a(u) \geq 0$, $r(u)$ and $g(q)$ are arbitrary functions, have been designed in [49]. The design of numerical fluxes follows the same lines as that for the

convection-diffusion equation (4.2) and for the KdV-type equation (5.3). A cell entropy inequality and the L^2-stability of the LDG scheme for the nonlinear equation (5.31) can be proved [49], which again do not depend on the smoothness of the solution of (5.31) and the order of accuracy of the scheme. The LDG scheme is used in [49] to study different regimes when one of the dissipation and the dispersion mechanisms dominates, and when they have comparable influence on the solution. An advantage of the LDG scheme designed in [49] is that it is stable regardless of which mechanism (convection, diffusion, dispersion) actually dominates.

5.2.5 The Fifth-Order KdV-Type Equations

LDG methods for solving the fifth-order KdV-type equations

$$u_t + f(u)_x + (r'(u)g(r(u)_x)_x)_x + (s'(u)h(s(u)_{xx})_{xx})_x = 0, \tag{5.32}$$

where $f(u)$, $r(u)$, $g(q)$, $s(u)$ and $h(p)$ are arbitrary functions, have been designed in [49]. The design of numerical fluxes follows the same lines as that for the KdV-type equation (5.3). A cell entropy inequality and the L^2-stability of the LDG scheme for the nonlinear equation (5.32) can be proved [49], which again do not depend on the smoothness of the solution of (5.32) and the order of accuracy of the scheme. The LDG scheme is used in [49] to simulate the solutions of the Kawahara equation, the generalized Kawahara equation, Ito's fifth-order KdV equation, and a fifth-order KdV-type equations with high nonlinearities, which are all special cases of the equations represented by (5.32).

5.2.6 The Fully Nonlinear $K(n, n, n)$ Equations

LDG methods for solving the fifth-order fully nonlinear $K(n, n, n)$ equations

$$u_t + (u^n)_x + (u^n)_{xxx} + (u^n)_{xxxxx} = 0, \tag{5.33}$$

where n is a positive integer, have been designed in [49]. The design of numerical fluxes follows the same lines as that for the $K(m, n)$ equations (5.30). For odd n, stability in the L^{n+1}-norm of the resulting LDG scheme can be proved for the nonlinear equation (5.33) [49]. This scheme is used to simulate compacton propagation in [49].

5.2.7 The Nonlinear Schrödinger (NLS) Equation

In [50], LDG methods are designed for the generalized nonlinear Schrödinger (NLS) equation

$$i\, u_t + u_{xx} + i\, (g(|u|^2)u)_x + f(|u|^2)u = 0, \tag{5.34}$$

the two-dimensional version

$$i\, u_t + \Delta u + f(|u|^2)u = 0, \tag{5.35}$$

and the coupled nonlinear Schrödinger equation

$$\begin{cases} i\,u_t + i\,\alpha u_x + u_{xx} + \beta\,u + \kappa v + f(|u|^2, |v|^2)u = 0 \\ i\,v_t - i\,\alpha v_x + v_{xx} - \beta\,u + \kappa v + g(|u|^2, |v|^2)v = 0, \end{cases} \tag{5.36}$$

where $f(q)$ and $g(q)$ are arbitrary functions and α, β and κ are constants. With suitable choices of the numerical fluxes, the resulting LDG schemes are proved to satisfy a cell entropy inequality and L^2-stability [50]. The LDG scheme is used in [50] to simulate the soliton propagation and interaction, and the appearance of singularities. The easiness of *h-p* adaptivity of the LDG scheme and rigorous stability for the fully nonlinear case make it an ideal choice for the simulation of Schrödinger equations, for which the solutions often have quite localized structures.

5.2.8 The Kadomtsev-Petviashvili (KP) Equations

The two-dimensional Kadomtsev-Petviashvili (KP) equations

$$(u_t + 6uu_x + u_{xxx})_x + 3\sigma^2 u_{yy} = 0, \tag{5.37}$$

where $\sigma^2 = \pm 1$, are generalizations of the one-dimensional KdV equations and are important models for water waves. Because of the x-derivative for the u_t term, the equation (5.37) is well posed only in a function space with a global constraint, hence it is very difficult to design an efficient LDG scheme which relies on local operations. In [51], an LDG scheme for (5.37) is designed by carefully choosing locally supported bases which satisfy the global constraint needed by the solution of (5.37). The LDG scheme satisfies a cell entropy inequality and is L^2-stable for the fully nonlinear equation (5.37). Numerical simulations are performed in [51] for both the KP-I equations ($\sigma^2 = -1$ in (5.37)) and the KP-II equations ($\sigma^2 = 1$ in (5.37)). Line solitons and lump-type pulse solutions have been simulated.

5.2.9 The Zakharov-Kuznetsov (ZK) Equation

The two-dimensional Zakharov-Kuznetsov (ZK) equation

$$u_t + (3u^2)_x + u_{xxx} + u_{xyy} = 0 \tag{5.38}$$

is another generalization of the one-dimensional KdV equations. An LDG scheme is designed for (5.38) in [51] which is proved to satisfy a cell entropy inequality and to be L^2-stable. An L^2-error estimate is given in [53]. Various nonlinear waves have been simulated by this scheme in [51].

5.2.10 The Kuramoto-Sivashinsky-type Equations

In [52], an LDG method is developed to solve the Kuramoto-Sivashinsky-type equations

$$u_t + f(u)_x - (a(u)u_x)_x + (r'(u)g(r(u)_x)_x)_x + (s(u_x)u_{xx})_{xx} = 0, \tag{5.39}$$

where $f(u)$, $a(u)$, $r(u)$, $g(q)$ and $s(p) \geq 0$ are arbitrary functions. The Kuramoto-Sivashinsky equation

$$u_t + uu_x + \alpha u_{xx} + \beta u_{xxxx} = 0, \tag{5.40}$$

where α and $\beta \geq 0$ are constants, which is a special case of (5.39), is a canonical evolution equation which has attracted considerable attention over the last decades. When the coefficients α and β are both positive, its linear terms describe a balance between long-wave instability and short-wave stability, with the nonlinear term providing a mechanism for energy transfer between wave modes. The LDG method developed in [52] can be proved to satisfy a cell entropy inequality and is therefore L^2-stable, for the general nonlinear equation (5.39). The LDG scheme is used in [52] to simulate chaotic solutions of (5.40).

5.2.11 The Ito-Type Coupled KdV Equations

Also in [52], an LDG method is developed to solve the Ito-type coupled KdV equations

$$\begin{aligned} u_t + \alpha uu_x + \beta vv_x + \gamma u_{xxx} &= 0, \\ v_t + \beta(uv)_x &= 0, \end{aligned} \tag{5.41}$$

where α, β and γ are constants. An L^2-stability is proved for the LDG method. Simulation for the solution of (5.41) in which the result for u behaves like dispersive wave solution and the result for v behaves like shock wave solution is performed in [52] using the LDG scheme.

5.2.12 The Camassa-Holm (CH) Equation

An LDG method for solving the Camassa-Holm (CH) equation

$$u_t - u_{xxt} + 2\kappa u_x + 3uu_x = 2u_x u_{xx} + uu_{xxx}, \tag{5.42}$$

where κ is a constant, is designed in [54]. Because of the u_{xxt} term, the design of an LDG method is non-standard. By a careful choice of the numerical fluxes, the authors obtain an LDG scheme which can be proved to satisfy a cell entropy inequality and to be L^2-stable [54]. A sub-optimal $O(h^k)$ error estimate is also obtained in [54].

5.2.13 The Cahn-Hilliard Equation

LDG methods have been designed for solving the Cahn-Hilliard equation

$$u_t = \nabla \cdot \Big(b(u) \nabla \big(-\gamma \Delta u + \Psi'(u) \big) \Big), \tag{5.43}$$

and the Cahn-Hilliard system

$$\begin{cases} \boldsymbol{u}_t &= \nabla \cdot (\boldsymbol{B}(\boldsymbol{u}) \nabla \boldsymbol{\omega}), \\ \boldsymbol{\omega} &= -\gamma \Delta \boldsymbol{u} + D\Psi(\boldsymbol{u}), \end{cases} \tag{5.44}$$

in [47], where $\{D\Psi(\boldsymbol{u})\}_l = \frac{\partial \Psi(\boldsymbol{u})}{\partial u_l}$ and γ is a positive constant. Here $b(u)$ is the non-negative diffusion mobility and $\Psi(u)$ is the homogeneous free energy density for the scalar case (5.43). For the system case (5.44), $\boldsymbol{B}(\boldsymbol{u})$ is the symmetric positive semi-definite mobility matrix and $\Psi(\boldsymbol{u})$ is the homogeneous free energy density. The proof of the energy stability for the LDG scheme is given for the general nonlinear solutions. Many simulation results are given in [47].

In [48], a class of LDG methods are designed for the more general Allen-Cahn/Cahn-Hilliard (AC/CH) system in $\Omega \in \mathbb{R}^d$ $(d \leq 3)$

$$\begin{cases} u_t &= \nabla \cdot [b(u,v) \nabla (\Psi_u(u,v) - \gamma \Delta u)], \\ \rho v_t &= -b(u,v)[\Psi_v(u,v) - \gamma \Delta v]. \end{cases} \tag{5.45}$$

Energy stability of the LDG schemes is again proved. Simulation results are provided.

Bibliography

[1] D. Arnold, F. Brezzi, B. Cockburn and L. Marini, Unified analysis of discontinuous Galerkin methods for elliptic problems. *SIAM Journal on Numerical Analysis* **39** (2002), 1749–1779.

[2] H. Atkins and C.-W. Shu, Quadrature-free implementation of the discontinuous Galerkin method for hyperbolic equations. *AIAA Journal* **36** (1998), 775–782.

[3] F. Bassi and S. Rebay, A high-order accurate discontinuous finite element method for the numerical solution of the compressible Navier-Stokes equations. *Journal of Computational Physics* **131** (1997), 267–279.

[4] C.E. Baumann and J.T. Oden, A discontinuous *hp* finite element method for convection-diffusion problems. *Computer Methods in Applied Mechanics and Engineering* **175** (1999), 311–341.

[5] R. Biswas, K.D. Devine and J. Flaherty, Parallel, adaptive finite element methods for conservation laws. *Applied Numerical Mathematics* **14** (1994), 255–283.

[6] Y. Cheng and C.-W. Shu, A discontinuous Galerkin finite element method for time-dependent partial differential equations with higher order derivatives. *Mathematics of Computation* **77** (2008), 699–730.

[7] P. Ciarlet, *The Finite Element Method for Elliptic Problems*. North Holland, 1975.

[8] B. Cockburn, Discontinuous Galerkin methods for convection-dominated problems. In: *High-Order Methods for Computational Physics*, T.J. Barth and H. Deconinck, editors, Lecture Notes in Computational Science and Engineering, volume 9, Springer, 1999, 69–224.

[9] B. Cockburn, B. Dong and J. Guzmán, Optimal convergence of the original DG method for the transport-reaction equation on special meshes. *SIAM Journal on Numerical Analysis* **46** (2008), 1250–1265.

[10] B. Cockburn, S. Hou and C.-W. Shu, The Runge-Kutta local projection discontinuous Galerkin finite element method for conservation laws IV: the multidimensional case. *Mathematics of Computation* **54** (1990), 545–581.

[11] B. Cockburn, G. Karniadakis and C.-W. Shu, The development of discontinuous Galerkin methods. In: *Discontinuous Galerkin Methods: Theory, Computation and Applications*, B. Cockburn, G. Karniadakis and C.-W. Shu, editors, Lecture Notes in Computational Science and Engineering, volume 11, Springer, 2000, Part I: Overview, 3–50.

[12] B. Cockburn, S.-Y. Lin and C.-W. Shu, TVB Runge-Kutta local projection discontinuous Galerkin finite element method for conservation laws III: one dimensional systems. *Journal of Computational Physics* **84** (1989), 90–113.

[13] B. Cockburn and C.-W. Shu, TVB Runge-Kutta local projection discontinuous Galerkin finite element method for conservation laws II: general framework. *Mathematics of Computation* **52** (1989), 411–435.

[14] B. Cockburn and C.-W. Shu, The Runge-Kutta local projection P^1-discontinuous-Galerkin finite element method for scalar conservation laws. *Mathematical Modelling and Numerical Analysis* (M^2AN) **25** (1991), 337–361.

[15] B. Cockburn and C.-W. Shu, The Runge-Kutta discontinuous Galerkin method for conservation laws V: multidimensional systems. *Journal of Computational Physics* **141** (1998), 199–224.

[16] B. Cockburn and C.-W. Shu, The local discontinuous Galerkin method for time-dependent convection-diffusion systems. *SIAM Journal on Numerical Analysis* **35** (1998), 2440–2463.

[17] B. Cockburn and C.-W. Shu, Runge-Kutta Discontinuous Galerkin methods for convection-dominated problems. *Journal of Scientific Computing* **16** (2001), 173–261.

[18] B. Cockburn and C.-W. Shu, Foreword for the special issue on discontinuous Galerkin method. *Journal of Scientific Computing* **22–23** (2005), 1–3.

[19] C. Dawson, Foreword for the special issue on discontinuous Galerkin method. *Computer Methods in Applied Mechanics and Engineering* **195** (2006), 3183.

[20] S. Gottlieb and C.-W. Shu, Total variation diminishing Runge-Kutta schemes. *Mathematics of Computation* **67** (1998), 73–85.

[21] S. Gottlieb, C.-W. Shu and E. Tadmor, Strong stability preserving high order time discretization methods. *SIAM Reviews* **43** (2001), 89–112.

[22] A. Harten, High resolution schemes for hyperbolic conservation laws. *Journal of Computational Physics* **49** (1983), 357–393.

[23] G.-S. Jiang and C.-W. Shu, On cell entropy inequality for discontinuous Galerkin methods. *Mathematics of Computation* **62** (1994), 531–538.

[24] C. Johnson and J. Pitkäranta, An analysis of the discontinuous Galerkin method for a scalar hyperbolic equation. *Mathematics of Computation* **46** (1986), 1–26.

[25] P. Lesaint and P.A. Raviart, On a finite element method for solving the neutron transport equation. In: *Mathematical aspects of finite elements in partial differential equations*, C. de Boor, ed., Academic Press, 1974, 89–145.

[26] R.J. LeVeque, *Numerical Methods for Conservation Laws*. Birkhäuser, Basel, 1990.

[27] D. Levy, C.-W. Shu and J. Yan, Local discontinuous Galerkin methods for nonlinear dispersive equations. *Journal of Computational Physics* **196** (2004), 751–772.

[28] P.-L. Lions and P.E. Souganidis, Convergence of MUSCL and filtered schemes for scalar conservation law and Hamilton-Jacobi equations. *Numerische Mathematik* **69** (1995), 441–470.

[29] J.T. Oden, I. Babuvska and C.E. Baumann, A discontinuous *hp* finite element method for diffusion problems. *Journal of Computational Physics* **146** (1998), 491–519.

[30] S. Osher, Convergence of generalized MUSCL schemes. *SIAM Journal on Numerical Analysis* **22** (1985), 947–961.

[31] S. Osher and S. Chakravarthy, High resolution schemes and the entropy condition. *SIAM Journal on Numerical Analysis* **21** (1984), 955–984.

[32] S. Osher and E. Tadmor, On the convergence of the difference approximations to scalar conservation laws. *Mathematics of Computation* **50** (1988), 19–51.

[33] T. Peterson, A note on the convergence of the discontinuous Galerkin method for a scalar hyperbolic equation. *SIAM Journal on Numerical Analysis* **28** (1991), 133–140.

[34] J. Qiu and C.-W. Shu, Hermite WENO schemes and their application as limiters for Runge-Kutta discontinuous Galerkin method: one dimensional case. *Journal of Computational Physics* **193** (2003), 115–135.

[35] J. Qiu and C.-W. Shu, Runge-Kutta discontinuous Galerkin method using WENO limiters. *SIAM Journal on Scientific Computing* **26** (2005), 907–929.

[36] J. Qiu and C.-W. Shu, Hermite WENO schemes and their application as limiters for Runge-Kutta discontinuous Galerkin method II: two dimensional case. *Computers & Fluids* **34** (2005), 642–663.

[37] W.H. Reed and T.R. Hill, Triangular mesh methods for the neutron transport equation. Tech. Report LA-UR-73-479, Los Alamos Scientific Laboratory, 1973.

[38] J.-F. Remacle, J. Flaherty and M. Shephard, An adaptive discontinuous Galerkin technique with an orthogonal basis applied to Rayleigh-Taylor flow instabilities. *SIAM Review* **45** (2003), 53–72.

[39] G.R. Richter, An optimal-order error estimate for the discontinuous Galerkin method. *Mathematics of Computation* **50** (1988), 75–88.

[40] P. Rosenau and J.M. Hyman, Compactons: solitons with finite wavelength. *Physical Review Letters* **70** (1993), 564–567.

[41] C.-W. Shu, TVB uniformly high-order schemes for conservation laws. *Mathematics of Computation* **49** (1987), 105–121.

[42] C.-W. Shu, Total-Variation-Diminishing time discretizations. *SIAM Journal on Scientific and Statistical Computing* **9** (1988), 1073–1084.

[43] C.-W. Shu, A survey of strong stability preserving high order time discretizations. In: *Collected Lectures on the Preservation of Stability under Discretization*, D. Estep and S. Tavener, editors, SIAM, 2002, 51–65.

[44] C.-W. Shu and S. Osher, Efficient implementation of essentially non-oscillatory shock-capturing schemes. *Journal of Computational Physics* **77** (1988), 439–471.

[45] B. van Leer and S. Nomura, Discontinuous Galerkin for diffusion. 17th AIAA Computational Fluid Dynamics Conference (June 6–9, 2005), AIAA paper 2005–5108.

[46] Y. Xia, Y. Xu and C.-W. Shu, Efficient time discretization for local discontinuous Galerkin methods. *Discrete and Continuous Dynamical Systems – Series B* **8** (2007), 677–693.

[47] Y. Xia, Y. Xu and C.-W. Shu, Local discontinuous Galerkin methods for the Cahn-Hilliard type equations. *Journal of Computational Physics* **227** (2007), 472–491.

[48] Y. Xia, Y. Xu and C.-W. Shu, Application of the local discontinuous Galerkin method for the Allen-Cahn/Cahn-Hilliard system. *Communications in Computational Physics* **5** (2009), 821–835.

[49] Y. Xu and C.-W. Shu, Local discontinuous Galerkin methods for three classes of nonlinear wave equations. *Journal of Computational Mathematics* **22** (2004), 250–274.

[50] Y. Xu and C.-W. Shu, Local discontinuous Galerkin methods for nonlinear Schrödinger equations. *Journal of Computational Physics* **205** (2005), 72–97.

[51] Y. Xu and C.-W. Shu, Local discontinuous Galerkin methods for two classes of two dimensional nonlinear wave equations. *Physica D* **208** (2005), 21–58.

[52] Y. Xu and C.-W. Shu, Local discontinuous Galerkin methods for the Kuramoto-Sivashinsky equations and the Ito-type coupled KdV equations. *Computer Methods in Applied Mechanics and Engineering* **195** (2006), 3430–3447.

[53] Y. Xu and C.-W. Shu, Error estimates of the semi-discrete local discontinuous Galerkin method for nonlinear convection-diffusion and KdV equations. *Computer Methods in Applied Mechanics and Engineering* **196** (2007), 3805–3822.

[54] Y. Xu and C.-W. Shu, A local discontinuous Galerkin method for the Camassa-Holm equation. *SIAM Journal on Numerical Analysis* **46** (2008), 1998–2021.

[55] J. Yan and C.-W. Shu, A local discontinuous Galerkin method for KdV type equations. *SIAM Journal on Numerical Analysis* **40** (2002), 769–791.

[56] J. Yan and C.-W. Shu, Local discontinuous Galerkin methods for partial differential equations with higher order derivatives. *Journal of Scientific Computing* **17** (2002), 27–47.

[57] M. Zhang and C.-W. Shu, An analysis of three different formulations of the discontinuous Galerkin method for diffusion equations. *Mathematical Models and Methods in Applied Sciences* (M^3AS) **13** (2003), 395–413.

[58] Q. Zhang and C.-W. Shu, Error estimates to smooth solutions of Runge-Kutta discontinuous Galerkin methods for scalar conservation laws. *SIAM Journal on Numerical Analysis* **42** (2004), 641–666.

[59] Q. Zhang and C.-W. Shu, Error estimates to smooth solutions of Runge-Kutta discontinuous Galerkin method for symmetrizable systems of conservation laws. *SIAM Journal on Numerical Analysis* **44** (2006), 1703–1720.

[60] J. Zhu, J.-X. Qiu, C.-W. Shu and M. Dumbser, Runge-Kutta discontinuous Galerkin method using WENO limiters II: unstructured meshes. *Journal of Computational Physics* **227** (2008), 4330–4353.